Thermo-hydraulic Analysis of Helically corrugated geometry using Single phase and Hybrid Nanofluids

Submitted By

Ashraf Mustakim **S.M. Naqib-Ul-Islam**

180011134 180011221

Supervised By

Dr. Mohammad Monjurul Ehsan

Associate Professor

A Thesis submitted in fulfillment of the requirement for the degree of Bachelor of Science in Mechanical Engineering

Department of Mechanical and Production Engineering (MPE)

Islamic University of Technology (IUT)

June, 2023

Candidate's Declaration

This is to certify that the work presented in this thesis, titled, "**Thermo-hydraulic analysis of helically corrugated geometry using single phase and hybrid nanofluids**", is the outcome of the investigation and research carried out by me under the supervision of **Dr. Mohammad Monjurul Ehsan, Associate Professor, Islamic University of Technology**.

It is also declared that neither this thesis nor any part of it has been submitted elsewhere for the award of any degree or diploma.

Ashraf Mustakim

Student No: 180011134

S.M. Naqib-Ul-Islam

Student No: 180011221

RECOMMENDATION OF THE BOARD OF SUPERVISORS

The thesis titled "**Thermo-hydraulic analysis of helically corrugated geometry using single phase and hybrid nanofluids**" submitted by Ashraf Mustakim, Student No: 180011134 and S.M.Naqib-Ul-Islam, Student No: 180011221 has been accepted as satisfactory in fulfillment of the requirements for the degree of B Sc. in Mechanical Engineering **on 21st June, 2023.**

BOARD OF EXAMINERS

1. ---

   Dr. Mohammad Monjurul Ehsan (Supervisor)
   Associate Professor
   MPE Dept., IUT, Board Bazar, Gazipur-1704, Bangladesh.

2. ---

   Dr. Shamsuddin Ahmed (Examiner)
   Professor
   MPE Dept., IUT, Board Bazar, Gazipur-1704, Bangladesh.

Acknowledgement

All praise goes to Almighty Allah to whom we surrender ourselves, for granting us the ability to complete this work on time. Without His grace and guidance, it could have been more difficult.

We would like to convey our profound gratitude to Dr. Mohammad Monjurul Ehsan, Associate Professor, Department of Mechanical and Production Engineering, IUT for his constant encouragement, perseverance, patience, and vast expertise throughout all stages of this study.

We would also like to highly appreciate Mr. Musfequs Salehin, Lecturer, Bangabandhu Sheikh Mujibur Rahman Aviation and Aerospace University, for his unwavering support and guidance throughout this project.

Special thanks to Asif Iqbal Turja and Rifat Ahamed for their encouragement & modelling the complex 3D geometry in Solidworks used in this research.

Abstract

This research set out to look at the aspects of flow and convective heat transfer in helically corrugated pipes. The main goal is to evaluate the thermo-hydrodynamic performance of single and hybrid nanofluids in this modified shape at different Reynolds numbers and nanoparticle volume concentrations. With dimensional modifications as in helical pitch, corrugation shape at the inlet, different case studies were performed for comparison in heat exchanger performance. Assuming a uniform heat flux of 1000 W/m2, Realizable k-epsilon turbulence model was used in ANSYS-FLUENT-2020 R1 commercial software to carry out the simulations at Reynolds numbers ranging from 5000 to 20,000. The study makes use of computational techniques to evaluate the thermo-hydrodynamic capabilities of corrugation coupled with varying volume fractions (1-5%) of single phase nanofluids (Al_2O_3 and CuO) and hybrid nanofluid (1% Al_2O_3/Cu). For solution approximation and discretization with SIMPLE pressure-velocity coupling, the second-order upwind technique is applied. Among the case studies, a change in corrugation inlet shape depicted the maximum augmentation whereas in terms of corrugation pitch, the lowest pitch corrugated tube had a considerably superior performance. Due to the intricacy of the corrugations, which enhances heat transmission and pressure drop with large volume fractions, a higher Nusselt number results. The heat transfer coefficient for various nanoparticle compositions for the helically corrugated pipe was demonstrated to be 20–30% greater than for the smooth pipe. Considering the pressure drop penalty and the heat transfer increase in terms of performance evaluation criterion (PEC), the 1% Al2O3/Cu water hybrid nanofluid was found to be the best-acquitted working fluid in the corrugated pipe flow with a maximum thermal performance improvement of 26.5%. The study also shows that the gain in thermal efficiency steadily declined as the Re rose, but it increased with an increase in the volume concentration of the nanofluid.

Keywords:

Helically corrugated pipes; Convective Heat transfer; heat exchanger; volume fractions; hybrid nanofluid; PEC

Table of Contents

List of Tables:

List of Figures

Chapter 1: Introduction

1.1 Objectives

1. To increase the efficiency of the heat exchanger by enhancing the heat transfer rate and thus defining its thermal performance.
2. To utilize geometrical modifications to introduce secondary flows and unsteadiness to increase heat transfer.
3. To couple the modified geometry with the presence of different nanoparticles to the original base fluid.
4. Application of hybrid nanofluids for further assessment of the thermal performance of the test geometry.

1.2 Structure of the thesis

In this project, 3 cases have been studied for flow characterization and heat transfer enhancement using nano-fluids and hybrid nanofluids. All the cases have been compared in terms of thermo-hydraulic behavior.

Chapter 2: Literature Review

Heat exchangers are an integral part of thermal power plants, heating, refrigeration and essentially on waste heat recovery units. Numerous engineering fields and industries, including the nuclear industry, solar collectors, refrigeration systems, thermal engineering, and power plants, among others, use corrugated geometries. Due to its increased demand in various engineering applications, continuous and extensive efforts are being made by researchers in various fields to increase the heat transfer characteristics of heat exchangers. For effectively circulating the fluid streams, a balance between the heat transfer rate and pumping power requirements will allow the thermal performance of a heat exchanger to be defined. Appropriate methods such as optimization of materials and designs are to be selected to augment the performance of such devices as well as making them cost-effective [1]. Utilizing various corrugated geometries significantly increases the rate of heat transmission, emphasizing the importance of corrugation design in heat exchangers. Among the obvious techniques is the use of passive ways that have proven to be cheaper and easy to implement [2]. Different configuration shapes are used in passive techniques to improve heat transfer performance by utilizing modified surfaces or the use of extended surfaces to stir up the flow field, altering the flow pattern, causing the thermal boundary layer to break [3]. Research by Promvonge et al [4] has demonstrated that the utilization of vortex flow may greatly speed up the rate of heat transfer in channels. Fluid dynamics states that dimples, corrugations, baffles and other passive techniques disrupt the creation of boundary layers. As a result, channel turbulence and heat transmission are increased. Thermal performance is improved by continually increasing the effective surface area and adding flow fields to the wall for circulation and recirculation [5]. Corrugated tubes provide higher ridges and the recirculating areas occur inside the grooves providing enhanced heat transfer and increased friction factor [6]. The thermal performance of corrugated pipes are better compared to smooth pipes [7]. The usage of helically corrugated tubes for heat exchanger design also has certain benefits. For example, their manufacturing costs are quite alike to those of a plain uncorrugated tube, and when compared to other types of modified geometries, their fouling removal is very simple. Thus, the purpose of this paper is to increase the efficiency of heat exchangers by utilizing geometrical modifications in to the tubes.

2.1 Effect of Corrugation

Passive techniques utilize geometrical modifications such as different shapes, (V- shaped) [8] joint turbulators and extended surface features [9], fins, twisted tapes or wired coil inserts, dimpled pipes [10], different type of ribs (curved, trapezoidal) [11] and even corrugated diameter rings [12] that improve heat transfer and pressure drop. Chudnovsky and Kozlov [13] used several flow obstruction shapes for the same working fluid to test the thermohydraulic performances. These geometries include riblets, wavy tubes, grooves, spiral grooves, finned tubes, and dimpled tubes. Such complexities in the geometry create agitation in the flow field by altering the flow pattern and breaking the thermal boundary layer. Under varying parameters, such geometries result in uneven thermal boundary layer distributions that increase separation and mixing resulting in enhancing the thermal flow performance. For turbulent flow condition, a study was performed numerically by M.M.Ali et al [14] for determining the impact of corrugation in the properties of working fluid. Results depicted enhanced performances in various shaped passages with a greater pressure loss as a result of the corrugations. Jayakumar et al. [15] studied the heat transfer mechanism in a helical coil heat exchanger both numerically and experimentally and found out that constant wall flux boundary condition has been a better assumption rather than constant wall temperature. Diameter, length, obstacles in the flow direction, coolant- these elements also influence the performance of a heat exchanger. Verma et al. [16] tested the effect of inserting a helical coil in the heat exchanger and found out that by using them the Nu number augmented by up to 2.64 times. Khosravi-Bizhaem et al [17] did an experimental study to analyze the effect of pulsation flow in a helical tube and found out by ways of pulsation flow heat transfer coefficient would have an increase of up to 39% and pressure drop increased by up to 7%. Zhang et al. [18] took into consideration a corrugated helical Heat exchanger. They determined that when the mass flow rate increases, the PEC value steadily rises, and the optimal value is found to be 0.35 kg/s to give optimum functioning.

2.2 Effect of Nanofluids

Nanotechnology has been in the works as a unique method in many engineering and industrial applications [19]. Small metal particles uniformly suspended in conventional base fluid like water, ethylene glycol etc are referred to as nanofluids [20]. Due to the presence of metal in these fluids, which may be utilized in parabolic collectors to maximize the utilization of solar energy, they have a high heat transfer coefficient [21]. Incorporating modified geometries with the presence of nanoparticles to the original working fluid is an example of a hybrid passive approach. With varying volume fractions, they offer enhanced, superior thermophysical qualities that result in increased thermal conductivity for the working fluid's remarkable thermal performance. The availability of ultra-fine particles brings higher stability contributing significantly into enhancement of local heat transfer coefficient [22]. Greater viscosity results in greater pressure drop and greater pumping force. Thus the incorporation of different nanofluids was set up. The coupling of nanofluids to the original working fluid for these complex geometries has proven to give enhanced results. When nanoparticles are added to the working fluid, the amount of turbulence that results rises [23]. Experimental research on nanofluid heat transfer within a straight tube with helically corrugated walls was conducted by Rabienataj Darzi et al. [24] .The researchers looked at a variety of factors, including the height and pitch of the corrugations. They discovered that adding nanoparticles to helically corrugated tubes increases their efficiency compared to plain tubes and that using nanofluid and helically corrugated tubes simultaneously can increase heat transmission by up to 320%. Srinivas and Vinod [25] investigated the effect of the Al_2O_3/water nanoparticles on the performance of a helical pipe and found out that the increase of flow rate increases the energy saving heavily. Biswakarma et al. [26] worked with helically v-grooved absorber tubes and results showed that using a nanofluid with an increase in Al2O3 content from 3% to 8% increased pressure drop by 14.5% and heat transfer coefficient by up to 13.8% when compared to the base fluid when operating at heat flux of 1000 W/m2 and Re = 4000. Abed et al. [27] performed computational simulations for a solar collector and results portrayed that Nusselt number of the single-phase fluid was increased by 32.4% for SiO2 with a volume fraction (VF) of 6%, with an improvement in thermal efficiency of 5.11% and a PEC of 1.313. Cázares et al. [28]

used nanofluids on solar collectors and their findings demonstrated that greater volume fraction nanofluids would have a stronger impact on enhancing the performance of the system and will boost it by as much as 80%.

2.3 Effect of hybrid nanofluids

The introduction of hybrid nanofluids combined both the simultaneous physical and chemical characteristics of many materials and displays the characteristics in a homogenous phase. These hybrid materials exhibit further improved thermo-physical properties that are said to have remarkable results. Due to the combination of several particles that enable the formation of adequate thermal interfaces within the fluid flow, other studies have also shown a considerable improvement in the heat transfer capacities of hybrid nanofluids [29]. Thus, the application of such hybrid nanofluids is implemented in this study to further evaluate the thermal performance of the test geometry. Regarding hybrid nanofluids, Ahmed A. Hussein et al added GNPs to different concentrations of MWCNTs and achieved 43.4% increase in heat transfer with an 11% rise in pressure drop. Alireza Akhgar et al [30] used TiO_2/MWCNT in water-ethylene glycol and got a maximum of 38.7% increase in thermal conductivity. When compared to employing 3% volume fractions of either TiO2-Oil or Al2O3-Oil alone, Bellos et al.'s [28] research shown that using 1.5% volume fractions of Al2O3 and TiO2 distributed in Oil increased thermal efficiency by more than two times. Ratul et al. [31] used 1% Al2O3-Cu/water nanofluid on dimpled channels and got a 2.67 times enhancement in thermal efficiency at Re of 5000. Foyez et al. [10] achieved 20.6% gain in thermal performance utilizing 3% Al2O3–CuO/ water hybrid nanofluid on double-dimpled pipe flow.

2.4 Research scope and problem statement

For the design of efficient and highly functioning heat exchangers, the utilization of hybrid passive technique which comprises of geometrical modifications coupled with nanoparticles into the working fluid has been a very useful approach from the aforementioned literatures. This study focused on applying this method by incorporating such a unique type of helical corrugation and use nanofluids as coolants for system optimization.

The thermo-hydrodynamic performance of heat exchangers is based on having a balance between heat transmission and pressure drop (ultimately pumping power) to get an optimized condition. With lesser research and assessment being done based on PEC of hybrid nanofluids in helically corrugated geometries of various configurations, this study proposed to enhance the heat transfer characteristics and improve the functions of a heat exchanger.

Different performance parameters such as heat transfer enhancement, pressure drop, friction factor, pumping power, wall shear stress, TKE and PEC have been computed in this study to identify which type of corrugation fits best for the design of heat exchangers. In order to further evaluate the performance of different concentrations of nanofluids (CuO/water, Al2O3/water, and hybrid nanofluids (Al2O3/Cu water), the research makes use of computational approaches. With increasing Re number the different characteristics are compared to make a conclusion on what turbulent regime of flow, the system performs optimally. The results of this study can be used to direct future research in the direction of creating corrugated tube designs that maximize heat transmission.

Nomenclatures and symbols

Abbreviation	**Meaning**	**Subscript**	**Meaning**
A_c	Cross-section area [m^2]	bf	Base fluid
Cp	Fluid specific heat capacity [J/(kg. K)]	nf	Nanofluid
D_h	Hydraulic diameter [m]	hnf	Hybrid nanofluid
D_o	Outer diameter [m]	np	Nanoparticle
e	Corrugation height [m]	avg	Average quantity
h	Convective heat transfer coefficient [$W/(m^2 .K)$]	In	inlet
k	Thermal conductivity [W/(m. K)]	Out	Outlet
L	Corrugated length [m]		
Nu	Nusselt number		
p	Corrugation pitch [m]	**Greek Symbol**	**Meaning**
p_w	Wetted perimeter [m]	ρ	Fluid density [kg/m^3]
PEC	Performance Evaluation Criterion	μ	Dynamic viscosity [kg/m.s]
Re	Reynolds number	ϕ	Viscous dissipation function [s^{-2}]
TKE	Turbulence Kinetic Energy	Ø	Volume fraction
u_{avg}	Average axial velocity [m/s]		

Chapter 3: Thermo-physical properties of nanofluids and hybrid nanofluids:

The thermo-physical properties of nanofluids are mainly obtained based on classical models but they do not always give accurate values. Experimental data gave more accurate models for calculating and defining these properties.

The effective properties of the water based nanofluid is given by Eqn. (1):

$$\rho_{nf} = \phi_p \rho_p + (1 - \phi)\rho_{bf} \quad (1)$$

This equation originated from [32] and has been used in several other literatures.

The density of hybrid nanofluids based on mixtures [33] is specified by Eqn. (2):

$$\rho_{hnf} = \phi_{p1}\rho_{p1} + \phi_{p2}\rho_{p2} + (1 - \phi)\rho_{bf} \quad (2)$$

With the density, volume fraction, and specific heat capacities of the base fluid and nanoparticles obtained, information on the specific heat capacity of nanofluids [34] is denoted by Eqn. (3):

$$C_{nf}\,\rho_{nf} = \phi_p \rho_p C_P + (1 - \phi)\rho_{bf} C_{bf} \quad (3)$$

For hybrid nanofluids, the heat capacity is given by Eqn. (4):

$$C_{hnf}\,\rho_{hnf} = \phi_{p1}\rho_{p1}C_{P1} + \phi_{p2}\rho_{p2}C_{P2} + (1 - \phi)\rho_{bf} C_{bf} \quad (4)$$

The Brinkman equation [35] is used to calculate the dynamic viscosity of nanofluids.

$$\mu_{nf} = \frac{\mu_{bf}}{(1 - \phi)^{2.5}} \quad (5)$$

And the viscosity for hybrid nanofluids is as follows:

$$\mu_{bf} = \mu_{hnf}\{(1-\phi_{p1})^{2.5}\left(1-\phi_{p2}\right)^{2.5}\} \quad (6)$$

The thermal conductivity of nanofluids is given by the Hamilton model [36]:

$$\frac{k_{nf}}{k_{bf}} = \frac{k_p + 2k_{bf} - 2\phi_p(k_{bf}-k_p)}{k_p + 2k_{bf} + \phi_p(k_{bf}-k_p)} \quad (7)$$

Thermal conductivity for hybrid nanofluids also resulted from Maxwell's equation [37]

$$\frac{k_{hnf}}{k_{bf}} = \frac{\frac{\phi_{p1}k_{p1} + \phi_{p1}k_{p1}}{\phi} + 2k_{bf} + 2\left(\phi_{p1}k_{p1} + \phi_{p2}k_{p2}\right) - 2\phi k_{bf}}{\frac{\phi_{p1}k_{p1} + \phi_{p1}k_{p1}}{\phi} + 2k_{bf} - \left(\phi_{p1}k_{p1} + \phi_{p2}k_{p2}\right) + \phi k_{bf}} \quad (8)$$

Table.1 exhibits the thermo-physical properties of the base fluid and the nanoparticles used in this study.

Table 1 Properties of base fluid and nanoparticles

Material	Density, ρ (kg/m3)	Heat capacity, Cp (J/Kg-K)	Thermal conductivity, k (W/m-K)	Dynamic viscosity, μ (kg/m-s)
Water	995.7	4178	0.615	0.0008
Al_2O_3	3970	775	39	0.000017
CuO	6510	540	18	0.0008

Chapter 4: Materials and Methods

4.1 Physical Model

Fig.1 represents a sketch of the 3D geometry of the helically corrugated pipe modelled in SolidWorks software. Three different views are represented in the figure for a complete look into the geometry. The corrugated walls are subjected to constant heat and its structural and dimensional characteristics are as follows: Total corrugation length of the pipe, L = 300mm. An additional 150mm of smooth pipe was modelled as the entry region before the corrugation region and a developing section of 450 mm smooth pipe length that allowed a fully developed hydrodynamic flow profile under almost adiabatic circumstances.

Additionally, the cross sectional area, Ac, and the corresponding wetted perimeter, P_w, are used to calculate the hydraulic diameter (Dh) of the corrugated pipe.

$$D_h = \frac{4A_c}{P_w} \qquad (9)$$

The inlet and outlet of the pipe is well named to be defined as the velocity inlet and pressure outlet, while the corrugated wall is exposed to constant heat flux of q = 1 kW/m2.

Understanding how various helical corrugation geometries affect pressure loss and heat transfer augmentation is the primary goal of the current effort. Therefore, different case studies were done on the internal flow in corrugated tubes having variable helical pitch and a change in the corrugation shape(trapezoidal) at the inlet but keeping the same outer diameter D_o and corrugation height e.

Table 2 lists the distinctive characteristics of the tested corrugated tubes (designated P12, P14, and P_{trap}), where a plain pipe with the same outside diameter was also taken into consideration as the reference geometry. The CAD model of the helically corrugated geometry is represented in the Figs (1,2 and 3) at different views to give a good visual understanding of this pipe.

Table 2 Design parameters of geometry:

Cases	**Outer diameter, D_o (mm)**	**Hydraulic diameter, D_h (mm)**	**Cross Sectional Area, A_c (mm^2)**	**Wetted Perimeter, P_w (mm)**	**Corrugation pitch, p (mm)**	**Corrugation height, e (mm)**
P12	5.5	5.1	15.06	13.85	12	0.4
P14	5.5	5.1	15.06	13.85	14	0.4
P_{trap}	5.5	4.75	21.43	18.04	12	0.4
Smooth	5.5	5.5	23.76	17.28	-	0.4

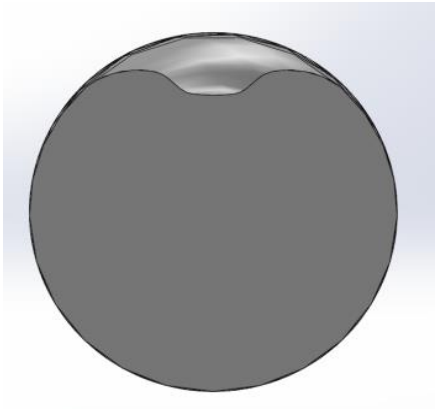

Figure 1 Inlet view

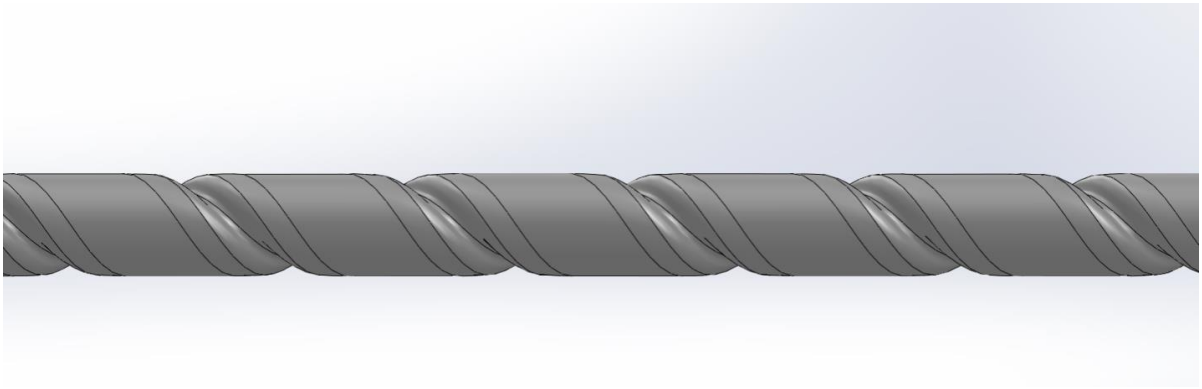

Figure 2 Side view

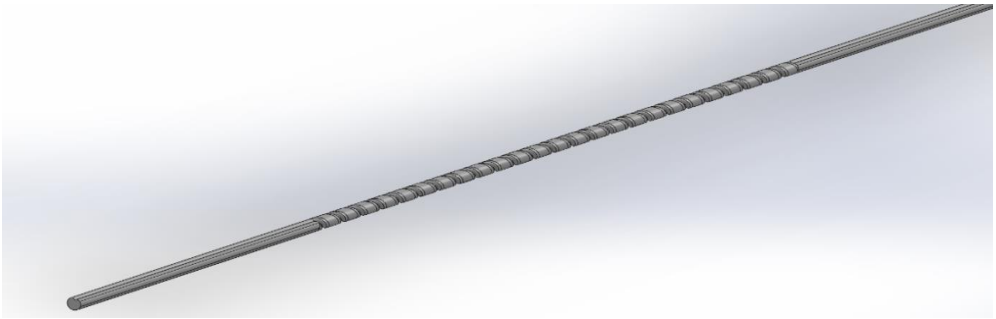

Figure 3 Isometric view

4.2 Mathematical Modelling and Assumptions:

This study is based on 3D incompressible flow inside corrugated pipes that requires the three major conservation equations (mass, momentum, energy) to be solved numerically with proper boundary conditions defined into the solver. The governing equations are as follows:

Mass: $\nabla.\left(\rho_f.V\right) = 0 \qquad where\ \rho = constant$ (10)

Momentum : $\rho.\left(\frac{\delta v}{\delta t} + v.\nabla v\right) = -\nabla P + \mu\nabla^2 v$ (11)

Energy: $\rho C_p\ (\left(\frac{\delta v}{\delta t} + v.\nabla T\right) = k\nabla^2 T + \mu^{\phi}$ (12)

where ϕ is the velocity dissipation function and v, T are the local velocity and temperature vectors respectively.

For this study, various assumptions were taken into consideration as our heat transfer is heavily influenced by forced convection.

• The working fluid is believed to be a Newtonian fluid and incompressible during the numerical studies.

• The thermo-physical properties of working fluids including hybrid nanofluids as well were taken to be constant and temperature independent.

• Heat loss to the environment is taken to be insignificant.

• Velocity from the inlet is considered to be uniform.

• Buoyancy effects are negligible as there is no natural convection effects.

4.3 Boundary Conditions:

At the intake region, flow velocity is computed using a temperature of 300 K, and turbulence intensity is determined using the Reynolds number.

$$I = 0.16Re^{-1/8} \quad (13)$$

The no-slip boundary phenomenon was specified to the pipe walls while an imposed heat flux of 1000W/m^2 was applied to the corrugated geometry. Using ANSYS fluent solver, the governing equations were numerically solved and during the pressure interpolation process, the Semi Implicit Method for Pressure-Linked Equations(SIMPLE) scheme was resolved for pressure-velocity coupling as it is the most convenient and robust method. Under the gradient portion, the Green-Gauss Node Based Method has been used for all calculations because it yields better logical answers while simultaneously consuming less CPU power [38]. Second-order upwind schemes and approximations were selected to discretize the continuity, momentum and energy equations as they are more accurate. Hybrid initialization was used since it solves a number of iterations (i=10) and provides a better estimate of the flow variables. ANSYS Workbench 2020 R1 was utilized throughout this study for all numerical simulations.

4.4 Performance Parameters:

The Reynolds number (Re), the average entry velocity (u_{avg}), and the pipe's intake and outside pressures are all specified as atmospheric pressure under the boundary conditions.

$$u_{avg} = \frac{\mu . Re}{\rho .\ D_h} \qquad (14)$$

The thermal assessment of convective heat transfer is conveyed by the non-dimensional Nuselt number, Nu:

$$Nu = \frac{h\ .D_h}{k} \qquad (15)$$

The equation below is used to obtain the pressure drop (ΔP) along the pipe from inlet to outlet.

$$\Delta P = P_{in} - P_{out} \qquad (16)$$

The pumping power per unit length in turbulent flow is given by:

$$W = \frac{\frac{\pi}{4} D_h^2\ u_{avg}\ \Delta P}{L} \qquad (17)$$

Where ΔP is the pressure drop along the pipe given by,

$$\Delta P = \frac{f\ L\ \rho\ u_{avg}^2}{2D_h} \qquad (18)$$

Wall shear stress at the corrugated wall is conveyed with:

$$\tau_o = \frac{f\ \rho\ u_{avg}^2}{8} \qquad (19)$$

The thermal-hydraulic performance of such layouts is assessed using the performance evaluation criterion (PEC). It is obtained by dividing the effect of considerable heat transmission by the increment in friction factor. Since water has a PEC value of one at all Re, nanofluids with PEC values larger than unity imply that heat exchanging characteristics outperforms that of air flow. This shows a greater thermal conductivity rating as compared to water [39]. The equation for PEC is given below.

$$PEC = \frac{(\frac{Nu_{nf}}{Nu_{bf}})}{(\frac{f_{nf}}{f_{bf}})\sqrt[3]{}} \qquad (20)$$

5. Numerical Implementation

5.1 Selection of Turbulence model:

The choice of a suitable turbulence model plays a key role in the accuracy of the complex geometry model's analysis. To dissect the flow characterization together with the heat transfer, simulations for the helically modified pipe are worked upon using both single phase and hybrid nanofluids. As this study dealt with fully turbulent region (Re =5000 to 20000), the Realizable k-epsilon model having enhanced wall treatment was employed as it is most commonly used for highly turbulent regimes. Some recent works have successfully applied this turbulence model [40]. In comparison to previous models, the Realizable k-epsilon model is able to compute internal forced convection solutions in tubes more precisely [41]. This turbulence model is suitable for issues with boundary layer distribution and flow separations. The momentum and turbulence equations were monitored as residuals having a convergence criterion of 10^{-6} in this study.

5.2 Mesh generation and grid independence test:

The CAD model was imported to ANSYS Fluent, where the fluid domain only is considered as the computational domain. The region of fluid flow is key for the mesh's computing effectiveness as well as its precision. The use of inflation layers with first layer thickness (y+ value) provided significant convergence results as it provides accurate computations and correctly captures the temperature and velocity gradients close to no-slip barriers. For a given flow regime, the y+ value, which denotes the non-dimensionalized near-wall grid spacing using shear stress velocity, is used to determine how coarse or fine a mesh is. The mid-section and cross-section views of the mesh are shown in Figs. 4 and 5.

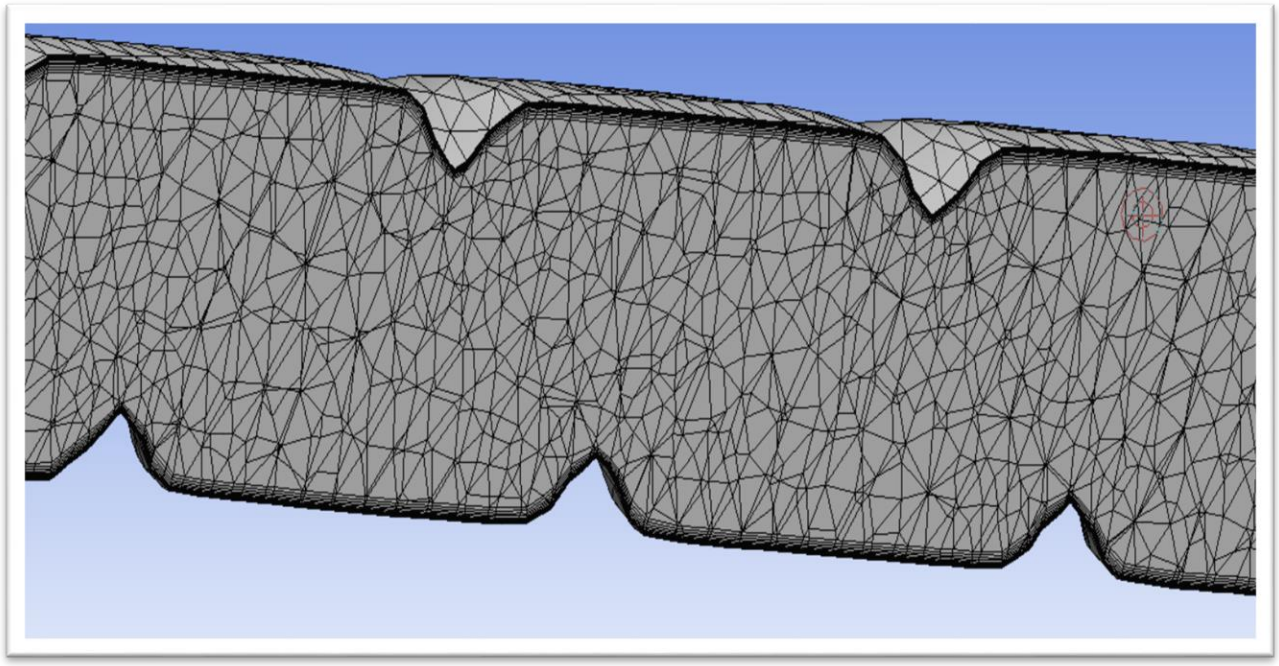

Figure 4 Mid-section view

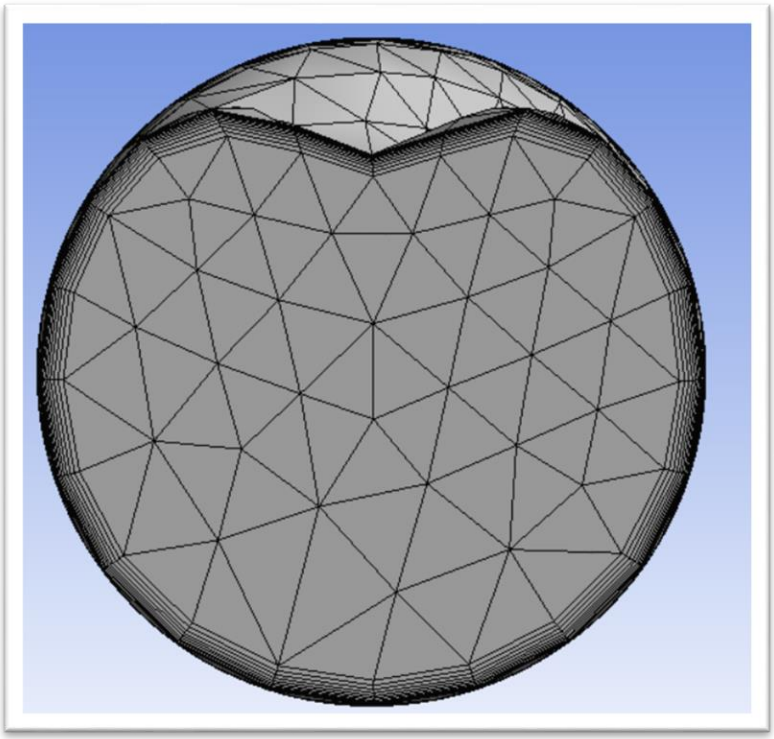

Figure 5 Cross section view

After finalizing the mesh, the grid independence studies are carried out prior to any further simulations to approach suitable and optimum cell size that gives the least amount of computational time. The corrugated pipe geometry is tested with different element sizes. Nusselt number values are numerically computed in various element sizes to see whether any noticeable variances are observed with respect to element numbers. Therefore numerous grid generations were carried out using 0.6 million to 1.24 million mesh components. Fig.6 depicts the Nu number variation with various element sizes at differing Reynolds number (5000 and 20000) to determine the optimum size with the least amount of variation. Approximately 880000 elements achieved a successful grid test. Thus this element size is used for further numerical analysis.

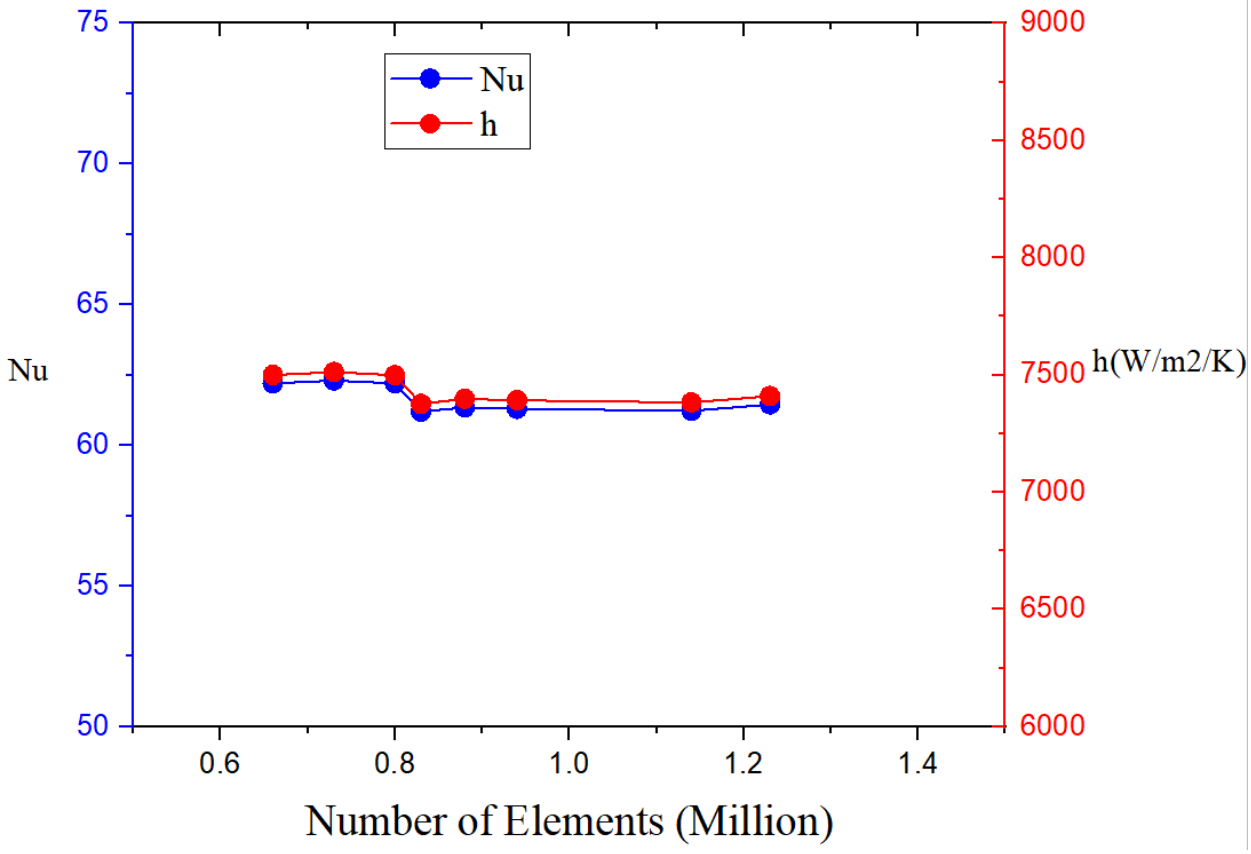

Figure 6 Variation of Nu number and heat transfer coefficient with number of elements for corrugated pipe at Re = 5000 and 20000.

6. Results and Discussion:

6.1 Model Validation

In order to determine the degree of trust in the outcomes, one must critically evaluate the early simulation forecasts. So, by solving the equation correctly and properly, the model was validated and confirmed. By contrasting the results with the produced experimental correlations of the researcher Presser [42], the constructed model's validity was ensured.

Presser Correlation:

$$Nu_{s,c} = \psi(Nu_{\infty}) \qquad (21)$$

Where $Nu = 0.023Re^{0.8}Pr^{0.4}$ and $\psi = 0.9217 + \frac{0.147P}{D} - 0.113e^{-7(\frac{P}{D}-1)}$

In Fig. 7, the present analysis is contrasted with the relationships that were previously discussed. The graphic demonstrates that, given a respectable margin of error, numerical findings fit all relationships well.

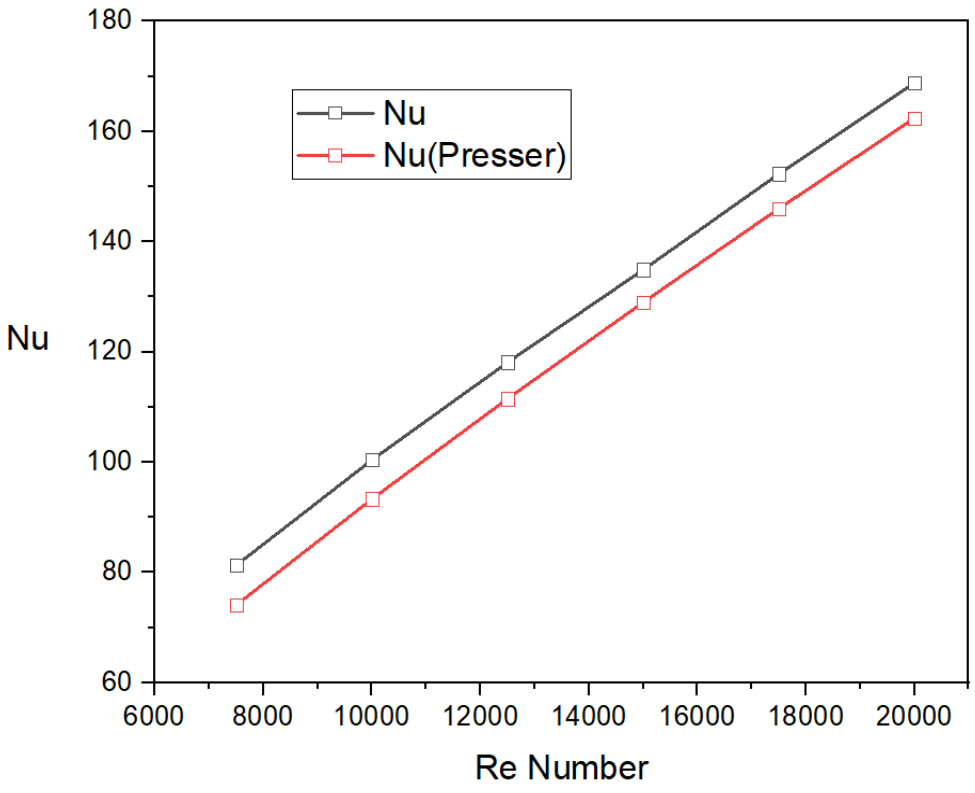

Figure 7 Model Validation

6.2 Thermo hydraulic performance analysis

6.2.1. Heat transfer characteristics

Thermo-physical properties based on Eq^{n}. (1-8) were used to obtain the values displayed in Table (3).

Table 3. Thermo-physical properties of water-based nanofluids at ϕ = 1% and hybrid nanofluids

Thermo-physical Properties	Al_2O_3	CuO	Al_2O_3/Cu hybrid
Density, ρ(kg/m^3)	1025.74	1051.04	1023.75
Heat capacity (J/kg-K)	4143.97	4141.47	4067.415
Thermal conductivity, k (W/m-K)	0.64173	0.632	0.65727
Viscosity (kg/m-s)	0.000858583	0.000858583	0.0016

From these values, the variation in Nu number is represented in the following Fig.8a for the number of different arrangements of corrugated pipe where the comparison is done using water and comparing all the three case studies along with the smooth pipe to determine the most suitable corrugation for optimum performance. It has been found out that the P_{trap} presents with the enhanced heat transfer coefficient by giving a Nu number of 178.3 at Re of 20000 whereas the Nu number was 168.8 and 161 for P12 and P14 respectively. With regards to the helical pitch, highest Nu number presents for geometry having the lowest pitch. This is supported by the corrugation obstacle's overwhelming influence on the boundary walls at higher Re numbers.In a more detailed manner, the multi-mode flow phenomenon that underlies the process of Nusselt number amplification superimposes the swirl effect on the flow separation and reattachment brought on by the corrugation itself. The Nusselt number enhancement quickly degrades when the boundary layer thickens as a result of the flow reattachment. The corrugation hurdle, however, encourages the periodic reconstruction of the boundary walls and allows enhancement by a smaller helical pitch leading to a more efficient heat transmission.

Fig.8b represents the variation of Nu number with 1% volume fractions of two nanofluids and a single hybrid nanofluid. Utilized on the geometry having a helical pitch of 12, for Re of 20000, the Nu of 1% Al_2O_3/Cu hybrid nanofluid is 23.2% higher than 1% Al_2O_3 nanofluid and 23.1% higher than 1% CuO nanofluid. Nanofluid possesses the superior thermophysical properties and so heat transfer rate increases significantly compared to water. Incorporating a tiny amount of Cu particle increases the thermal conductivity resulting in higher Nu number for hybrid nanofluids compared to single-nanofluid.

Fig.8c and d portrays the variation in Nu number at different volume fractions (1-5%) of both the water-based nanofluids (Al2O3 and CuO). With an increment in particles volume percentage and Reynolds number, adding these nano sized particles to the original fluid considerably enhances the convective heat transfer coefficients. There is a 15% increase in Nu number for 5% Al2O3 compared to 1% Al2O3.There is a 12.8% increase in Nu number for 5% CuO compared to 1% CuO.

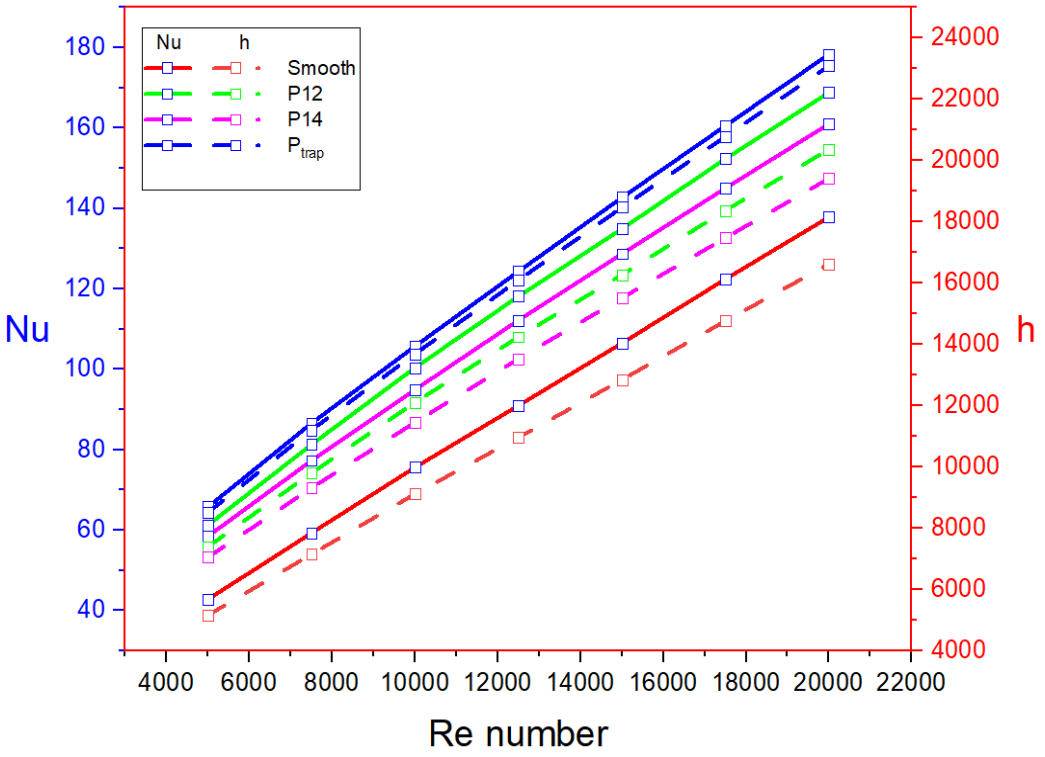

Figure 8a Variation of Nu number with Re number using water as working fluid for different geometrical configurations

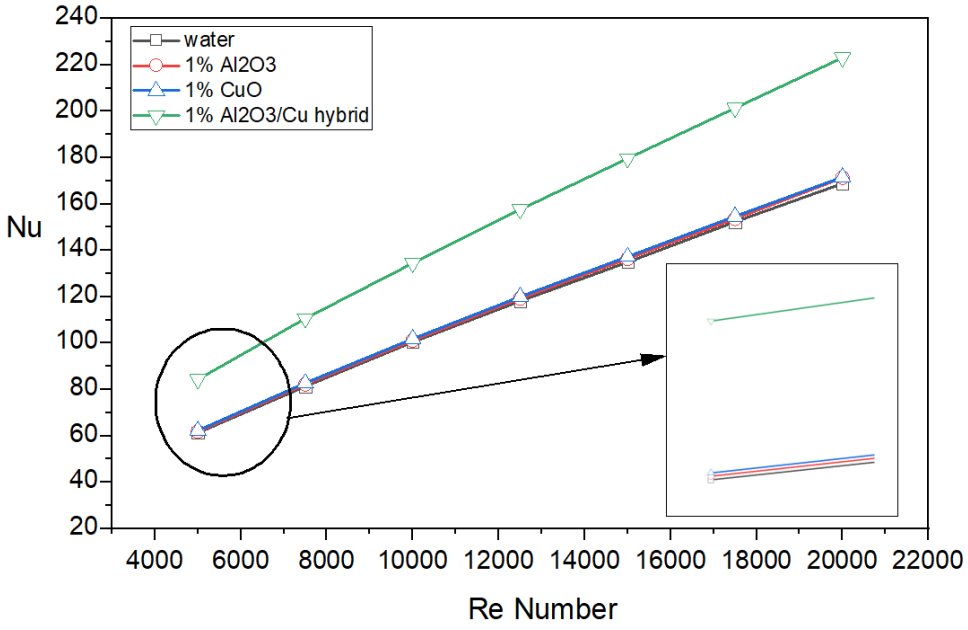

Figure 8b Variation of Nu number with Reynolds number using 1% volume fractions of nanofluids and hybrid nanofluid

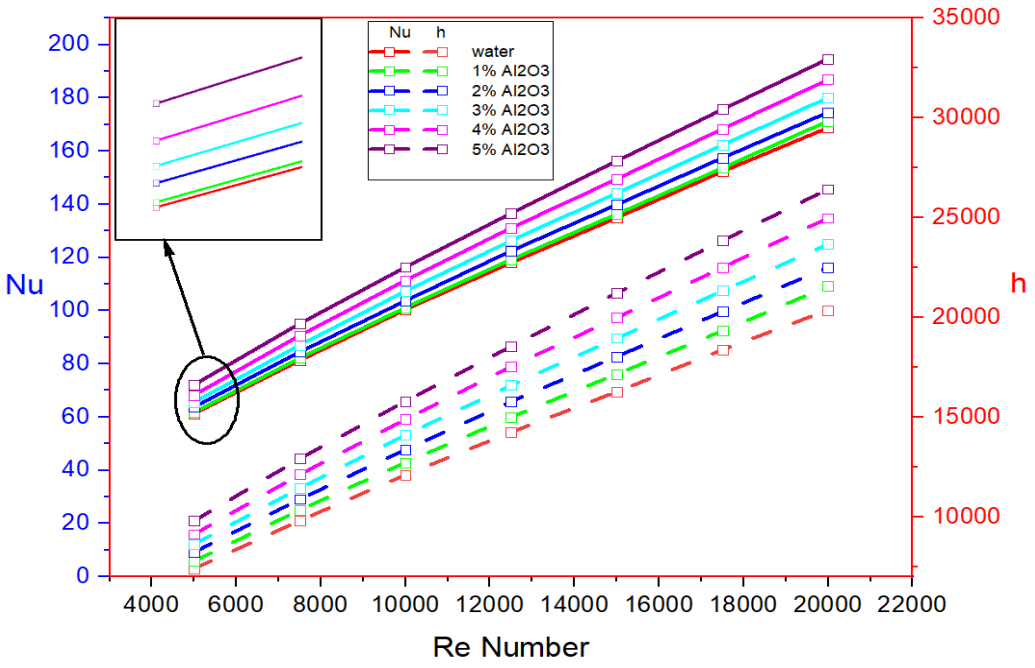

Figure 8c Variation of Nu number with Re number at (1-5%) volume fractions of Al2O3 nanofluid for P12.

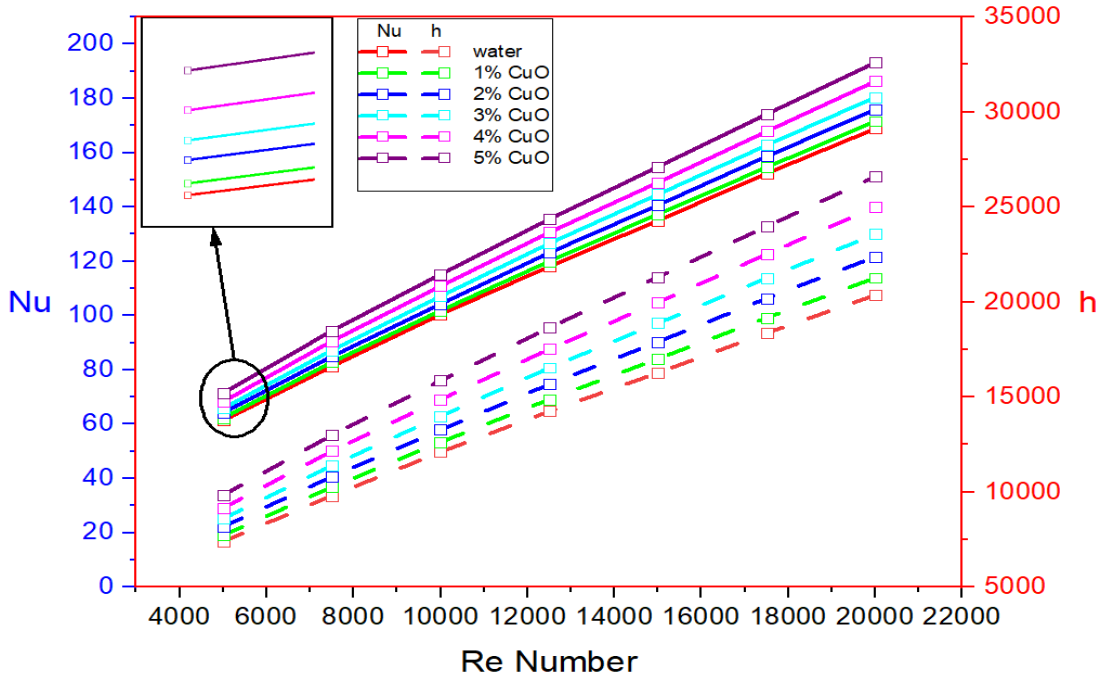

Figure 8d Variation of Nu number with Re number at (1-5%) volume fractions of CuO nanofluid for P12

6.2.2 Pressure drop analysis

As observed from fig.9, in comparison to a smooth tube, helical corrugation can significantly increase the friction factor, depending on the Reynolds number range of interest. All of the corrugated tubes behave as predicted in this regard. The model's display from Fig.9 show that the friction factor for the test geometry with pitch values of 12 and 14 clearly tends to decrease as the Reynolds number rises in the turbulent zone, which is in excellent accord with earlier findings published in the literature [43]. The corrugated pipe P_{trap} presents with the highest friction factor value.

Overall, the helical corrugation serves as a type of roughness which gets more exposed to the main flow as the Re number rises since it tends to be beyond the boundary layer. Reducing the pitch of the corrugations as a result increases the friction factor caused by normal stress.

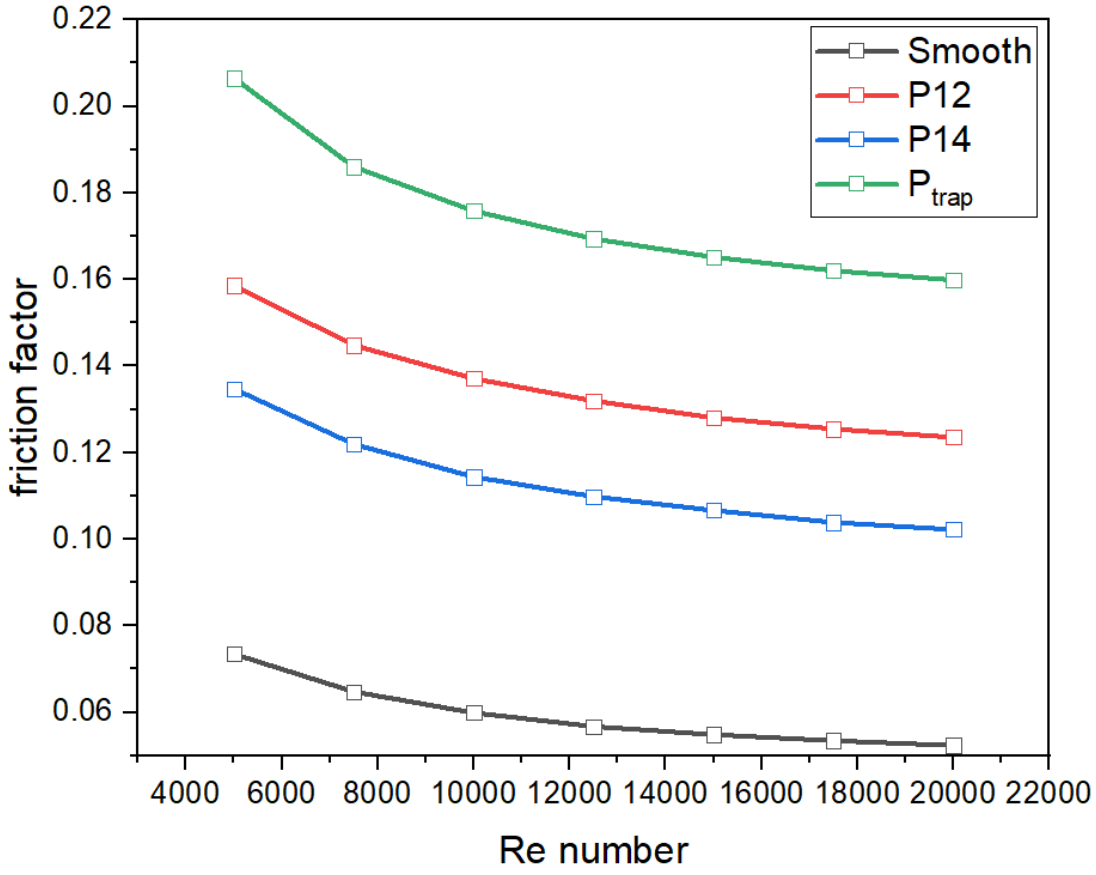

Figure 9 Variation of friction factor with Re number for different geometrical configurations

As previously mentioned, the use of nanoparticles enhances the thermal conductivity of the coolant. However, the inclusion of nanoparticles raises density and viscosity, causing a rise in pressure drop. Strong velocity gradients close to the wall create wall shear stress. The discrepancy in pressure drop across the analyzed geometries also gets worse as the Re rises. This happens because, as was already said, a higher Re number causes a bigger pressure decrease for a nanofluid. The pressure loss in the helically corrugated pipe is larger than in a smooth pipe due to abrupt changes in the velocity gradient and disturbance brought on due to corrugated parts. Due to the higher density and viscosity, a bigger pressure drop is seen as the nanofluid volume fraction increases. As fluid viscosity rises, this results in an increase in wall shear stress, as seen in Fig. 10. The thickness of the temperature and velocity boundary layers reduces as the Re gets closer, reducing the resistance the nanofluid experiences as it travels down the pipe.

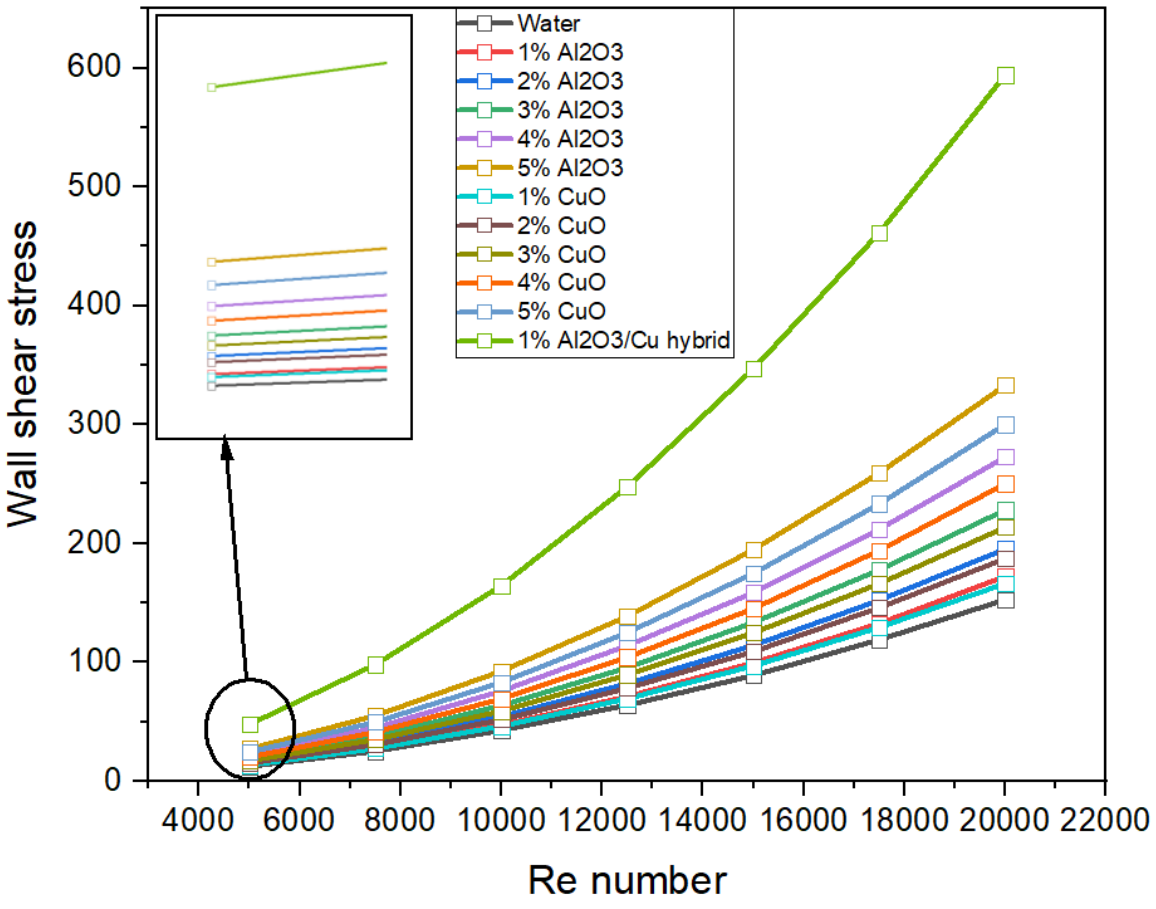

Figure 10 Variation of Wall shear stress with Re number for water, single phase nanofluids and hybrid nanofluid on P12

6.2.3 Pumping Power

The surface behavior of a pipe's interior is mostly responsible for pressure decrease. Due to a greater pressure drop, corrugated curved geometry demands more pumping power than circular pipe. With an increase in amplitude and wave duration, corrugation promotes flow separation and vortex production. Due to its near wall turbulence and more frictional losses, the required pumping power for corrugated pipe is more than that of plain pipe. Fig.11 depicts the pumping power requirements per unit length for all different geometrical configurations in this study.

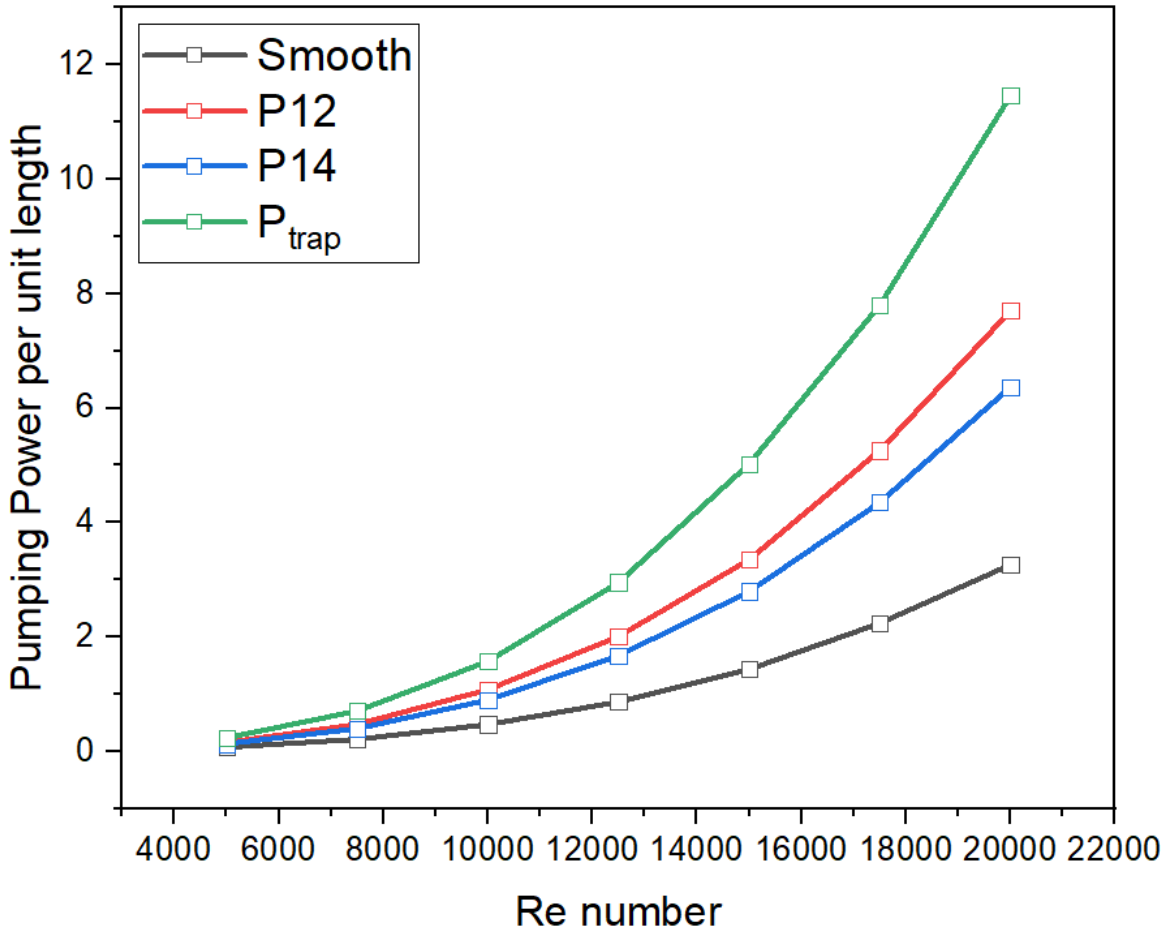

Figure 11 Pumping power with Re number for various geometrical configurations

Due to the working fluid's higher viscosity, as the concentration of nanofluid increases, more pumping power is needed. As per Fig. 12, Pumping power requirements for Al2O3-water and CuO-water nanofluid at 5% volume fraction are 66.75% and 59% higher, respectively, than for water flowing through a helically corrugated pipe in a turbulent regime with a Reynolds number of 20,000. The use of hybrid nanofluid requires even more pumping power for proper flow of the liquid through the pipe.

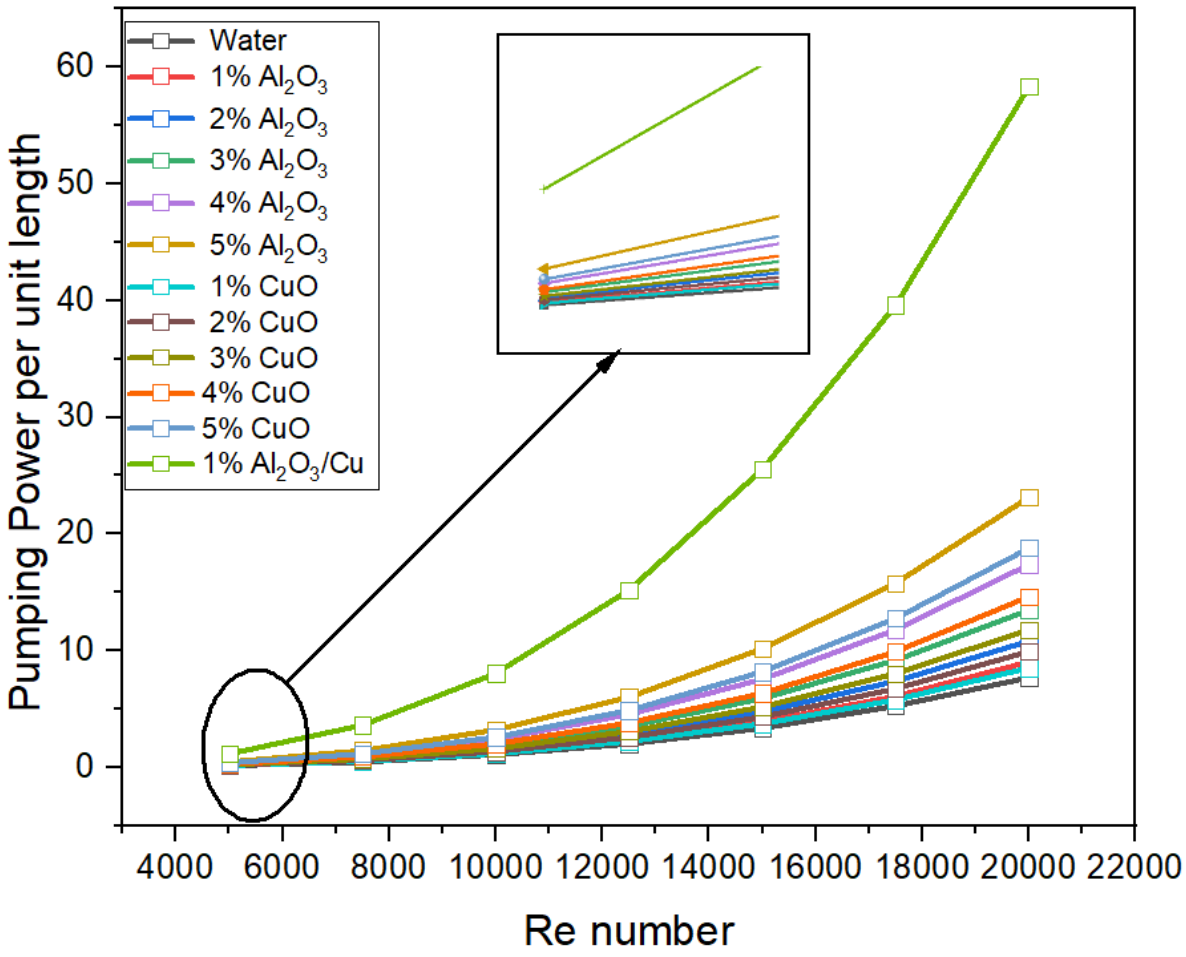

Figure 12 Pumping power with varying volume fractions of Al2O3, CuO and Hybrid nanofluid for P12 at Re = 5000 to 20000.

6.3 Flow behavior analysis

6.3.1. Pressure drop behaviour

Fig. 13a shows variations in pressure inside the corrugated tube when it is completely stretched. As the corrugated pipe's length moves forward, the pressure field within varies significantly and decreases sharply. There are major areas of concern in this flow field. The first region, located nearest to the inlet, has the highest pressure value. The second one, which is the middle portion, has a reduced pressure than the first one. The pressure value is rather low in the latter part.

Corrugation causes the boundary layer to break down, causing secondary flow and fluid recirculation. More variance in fluid flow may result from the phenomena. More mixing and swirls can be produced by faster flows, which can enhance turbulence and pressure drops.

As observed from Fig.13b and c, the utilization of nanofluids and hybrid nanofluids show a rise in pressure drop across the pipe compared to water as has been suggested in section 5.2.2. The average pressure drop increases gradually as the weight concentration rises due to the stronger cohesions between nanoparticles. The entry length's wall area experiences increasing velocity gradient and shear stress with rise in Re because it elongates the hydrodynamic entry length. As a result, the pressure drops in the entrance area grow, leading to an increase in the average pressure drop as Re rises.

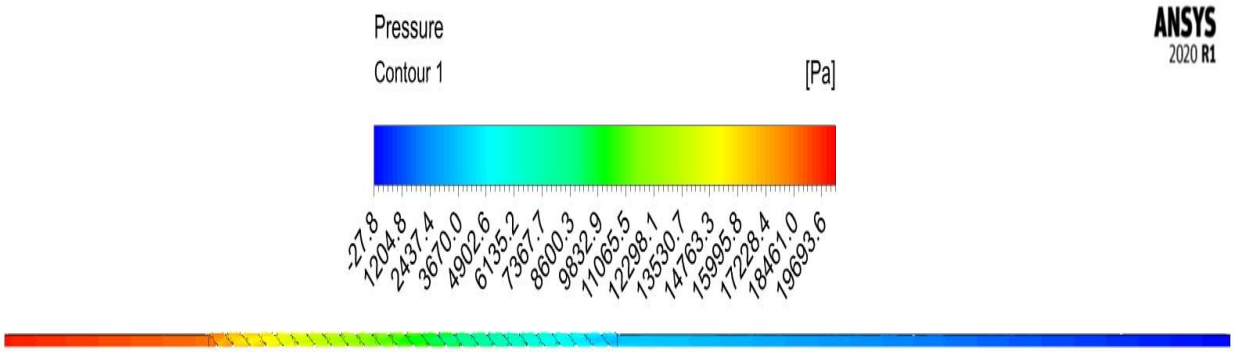

Figure 13a Pressure distribution along the corrugated pipe P12 using water at Re=10000

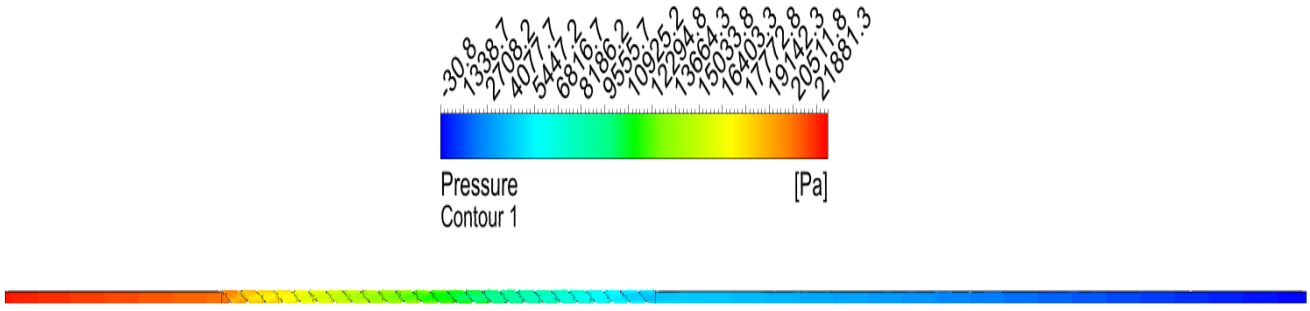

Figure 13b Pressure distribution along the corrugated pipe P12 using 1% Al2O3 nanofluid at Re=10000

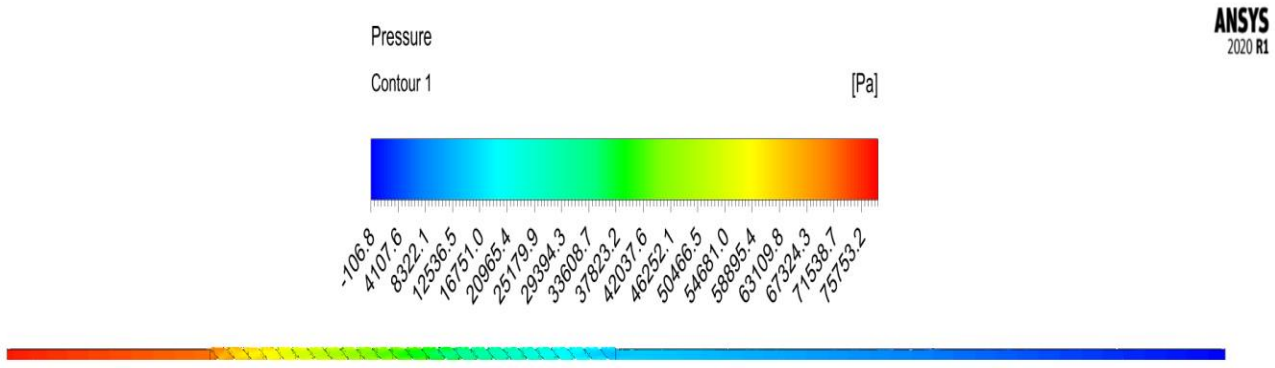

Figure 13c Pressure distribution along the corrugated pipe P12 using 1% Al2O3/Cu hybrid at Re=10000

6.3.2 Variation in flow velocity

In order to boost velocity, the inner flow area must be minimized since the corrugated surface has reduced the internal diameter of fluid flow. As shown in Fig.14a and b, the velocity distribution is expressed for two different helical pitch configurations (P12 and P14) of the corrugated geometry. Helical corrugation has two separate effects: it encourages swirl and produces artificial roughness by causing boundary layer fluctuations along the parallel flow of the pipe. The helical corrugation's ability to produce swirl is diminished at high pitches because it frequently conforms to fluid flow along the axis of the pipe. Contrarily, for low pitches, the corrugation mostly serves as a barrier, which causes the recirculation zone to widen and dampen the swirl effect.

Fig.14c depicts the velocity distribution for the corrugated region of P_{trap} geometry which is observed to have the highest velocity increment across the pipe due to the change in corrugation shape and also the reduced hydraulic diameter.

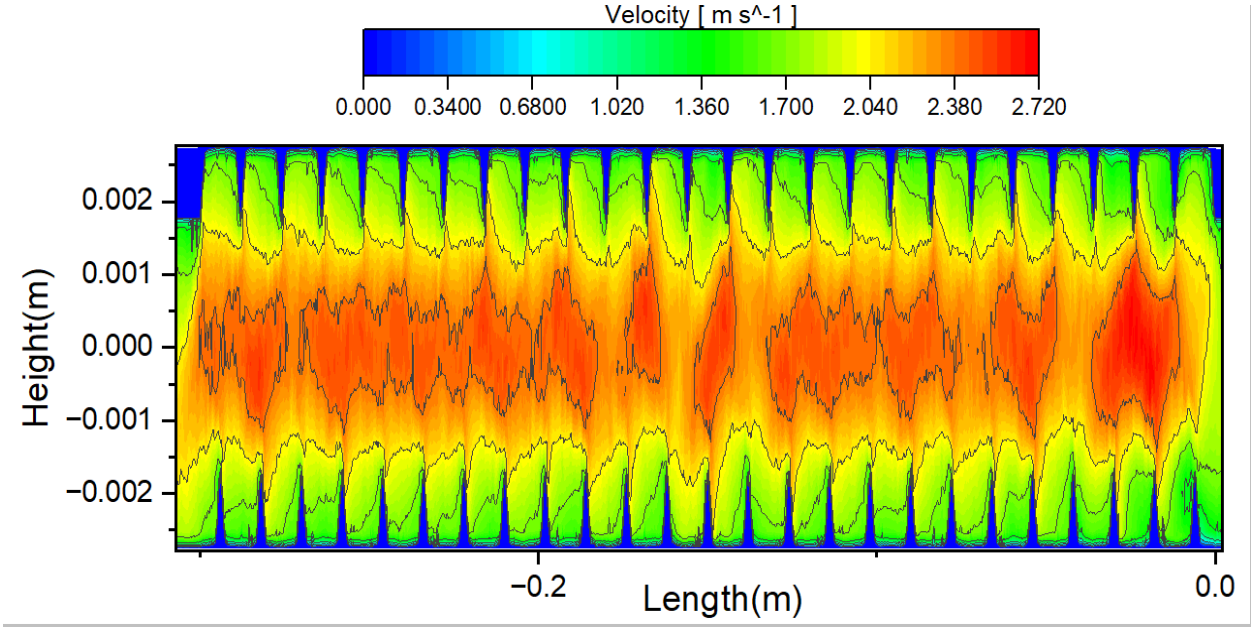

Figure 14a Velocity Contour at mid-section plane in corrugated region of P12 for water at Re=10000

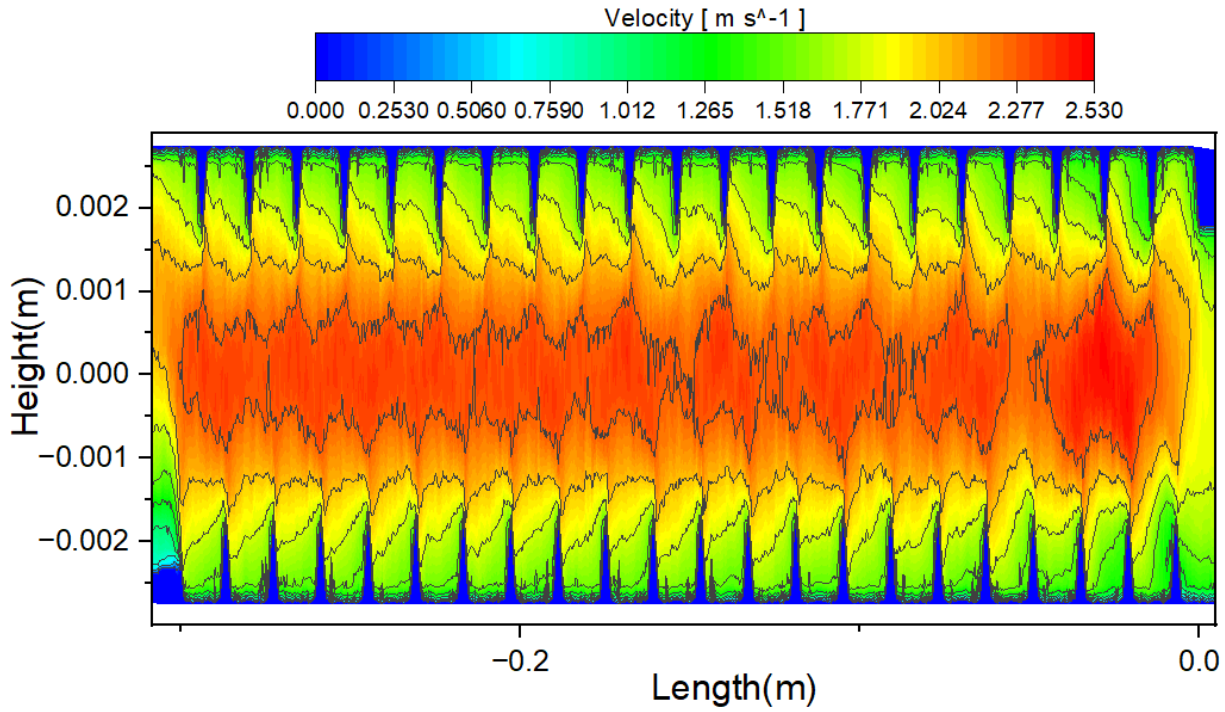

Figure 14b Velocity Contour at mid-section plane in corrugated region of P14 for water at Re=10000

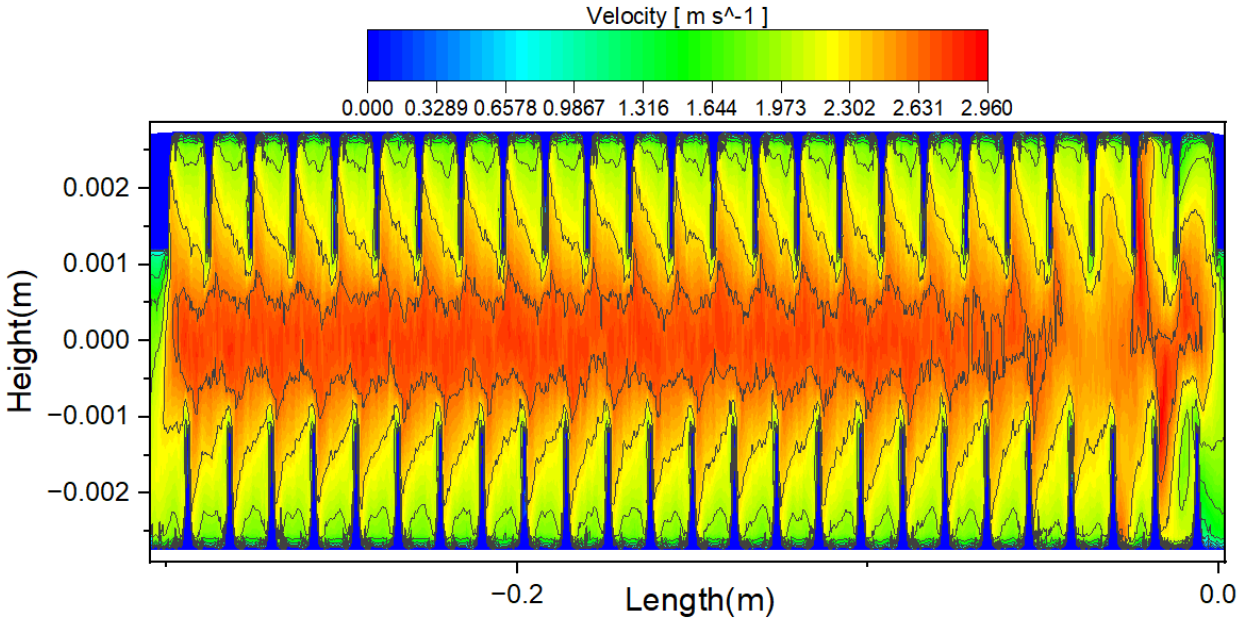

Figure 14c Velocity Contour at mid-section plane in corrugated region of P_{trap} for water at Re=10000

Fig. 15a, b, c represents the velocity distribution along the corrugated region for 3% Al2O3 nanofluid, 3% CuO nanofluid and 1% Al2O3/Cu hybrid nanofluid respectively. Water and nanofluid velocity patterns are qualitatively similar, however quantitatively, for 3% Al2O3 nanofluid, 3% CuO nanofluid and 1% Al2O3/Cu hybrid nanofluid they are not alike when compared to Figure 14a. The fundamental cause of this variance is the difference in buoyancy and viscous forces. Furthermore, compared to the base fluid water, the nanofluid's dynamic and thermal boundary layer is thicker due to its higher density and viscosity. Al2O3-Cu nanoparticles are added to water to create the nanofluid, which improves the fluid layers' intermixing and intensifies the secondary flow that is induced. This occurrence supports the hypothesis that velocity magnitude increases with increasing nanoparticle integration. Stronger velocity gradients are encouraged by the greater core velocities since they tend to spread to the area close to the wall.

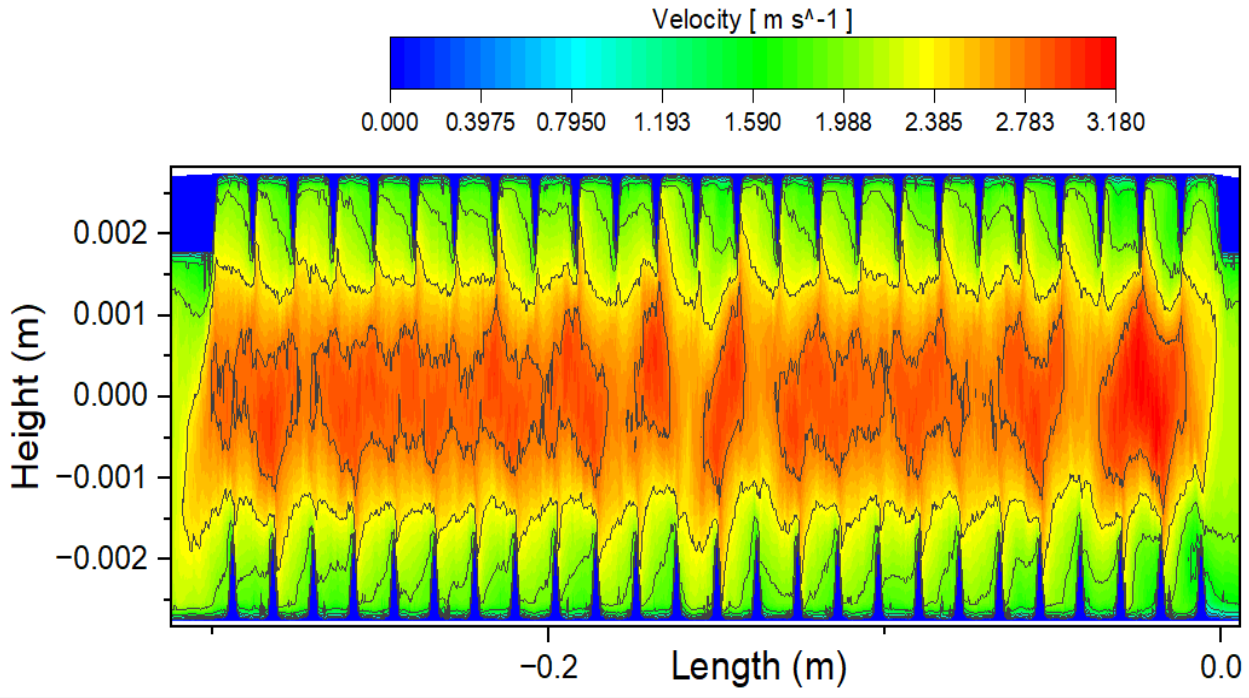

Figure 15a Velocity distribution contour of 3% Al2O3 nanofluid at Re=10000

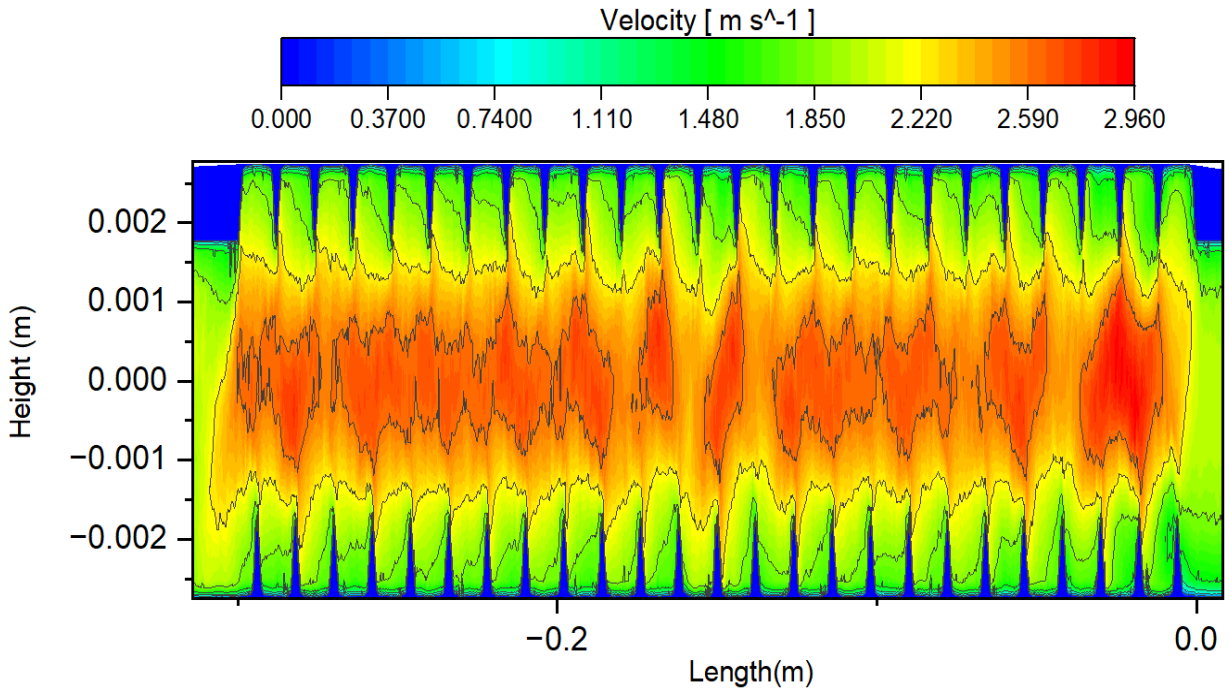

Figure 15b Velocity distribution contour of 3% CuO nanofluid at Re=10000

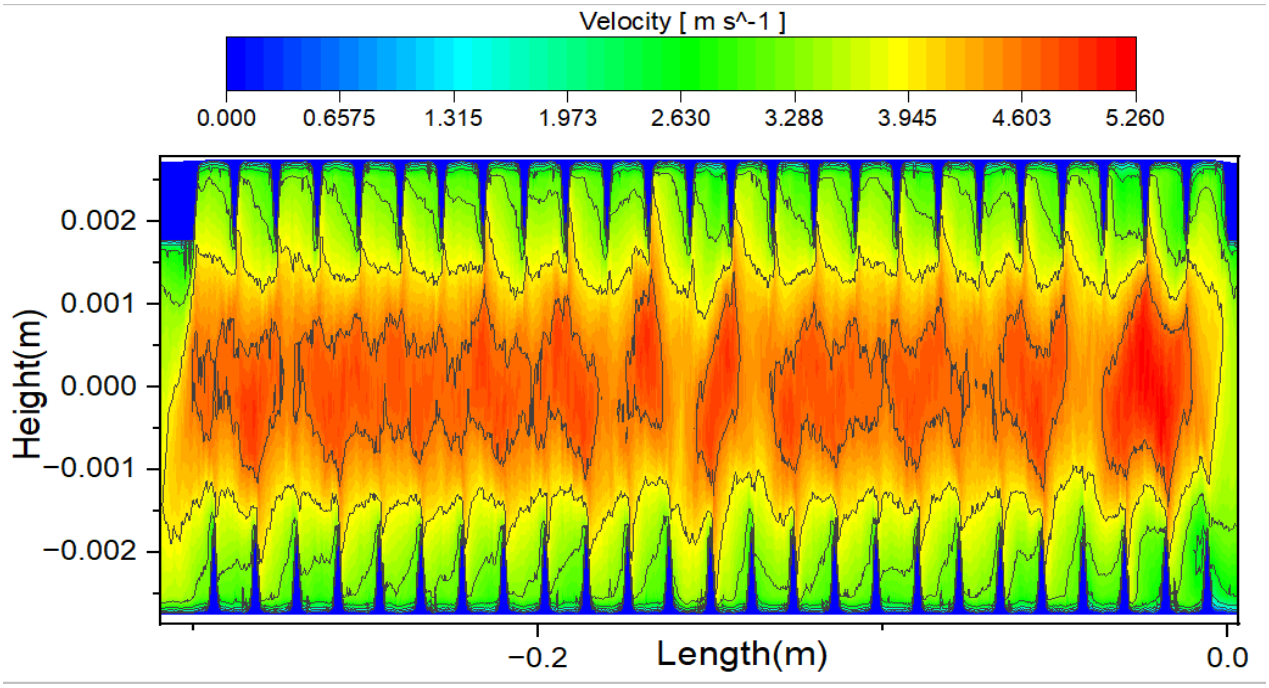

Figure 15c Velocity distribution contour of 1% Al2O3/Cu hybrid nanofluid at Re=10000

6.3.3 Performance evaluation criterion

Due to higher risks concerning large pressure drop, nanofluid's potential benefit in heat transmission must be assessed for thermal performance. Because the efficacy of cost and pressure drop are inherently linked, as the pressure drop goes up, so does the pumping power required and thus the performance evaluation criteria (PEC), which measures thermo-hydrodynamic performance, has been computed. PEC has a relationship with both the Nu and the friction factor; as a result, the value of PEC as a whole tends to decline as the Re increases. The improvement in heat transmission will be dominant over pressure loss if the PEC value is greater than 1. On the other hand, if the PEC value is less than 1, pressure drop will be larger than the improvement in heat transmission. The PEC of the Al2O3/Cu water hybrid nanofluid in various combinations is shown in Fig.16. From fig.16, The explanation and observation makes it obvious that, for all of the configurations that were analyzed, Re of 5000 had the greatest value of PEC discovered. As Re increased, the value of PEC decreased. Overall, it can be said that the corrugated tube having the lowest pitch (P12), at a fixed corrugation height, offers higher thermal performance for real-world applications. But the P_{trap} geometry gave the highest PEC value which makes it the optimum geometry in this study in terms of thermal performance. The Nusselt number ratio (Nu/Nu_o) has also been depicted in this figure.

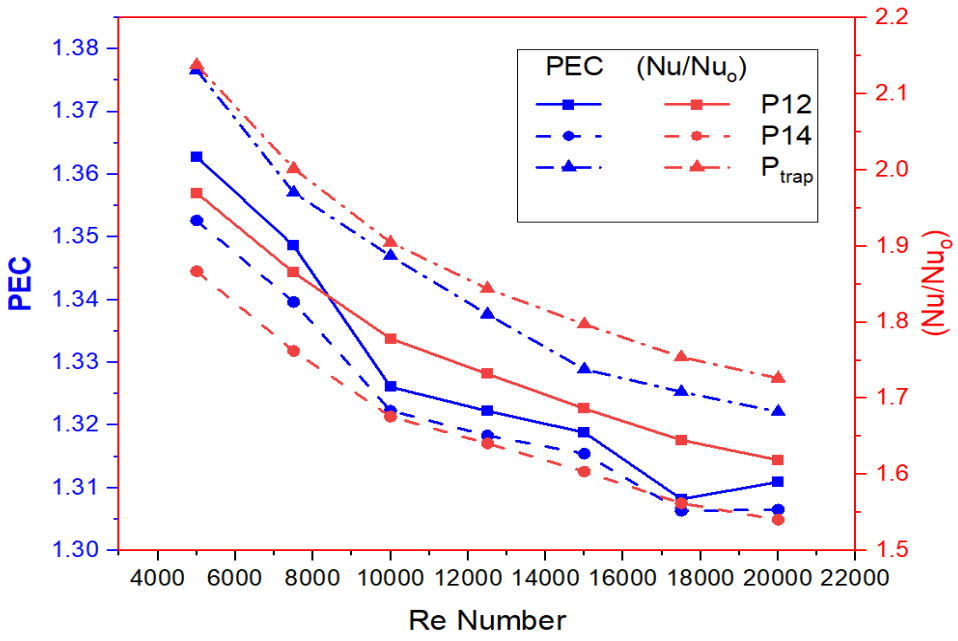

Figure 16 Variation of PEC and (Nu/Nu_o) for all three geometrical configurations with Re number using 1% Al2O3/Cu hybrid nanofluid

As the volume fraction of each nanofluid rises, the PEC value increases. This situation results due to a rise in density and pressure. Thus, the PEC value increases with increasing particle content for the present corrugated test segment. Fig.17 depicts PEC versus Re for the corrugated geometry(P12) for both the nanofluids with increasing concentrations.

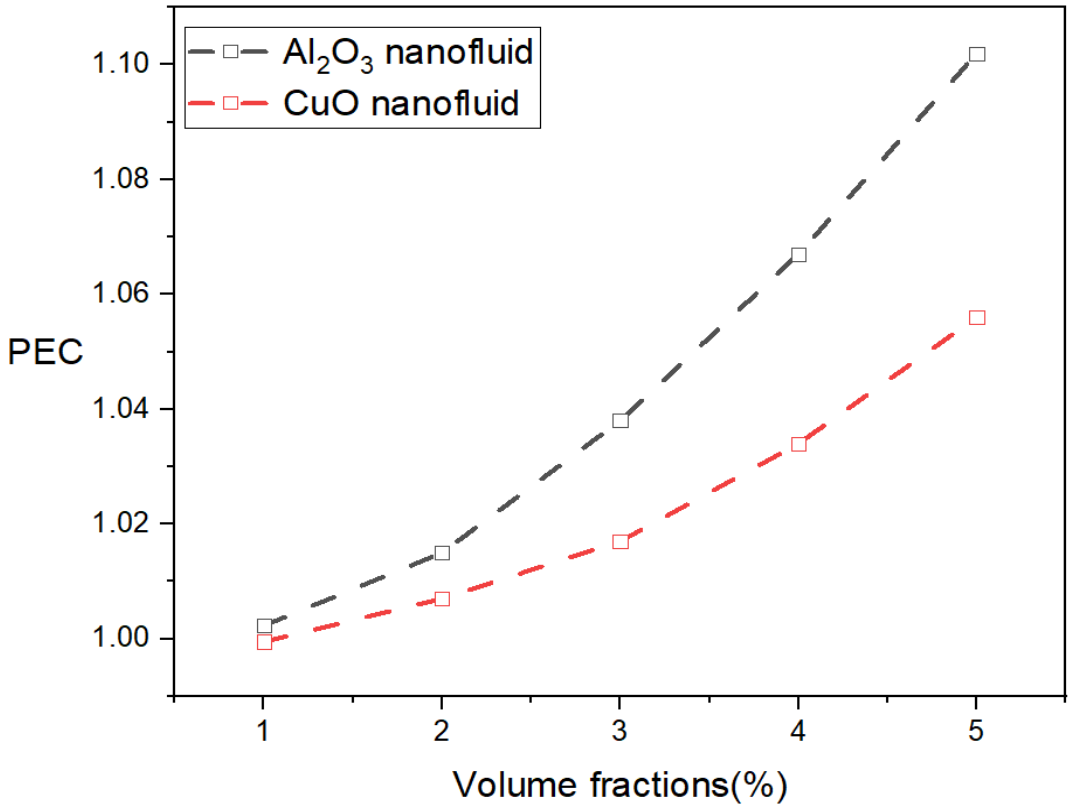

Figure 17 Variations in PEC for corrugated geometry (P12) at different volume fractions of nanofluids with Re number

6.3.4 Turbulence Kinetic Energy

Turbulent kinetic energy is a measure of the intensity of turbulence in a flow. The heat transfer coefficient would increase in value with a larger value of Turbulence intensity. Owing to the homogeneity of the flow, the quantity of TKE does not rise in a simple pipe as in Fig. 18a, but in the changed geometry, this amount will increase owing to the existence of corrugation, which will boost heat transfer as observed in Fig.18b. It is claimed that turbulence properties have the biggest influence on nanoparticle presence as depicted in Fig.18c.

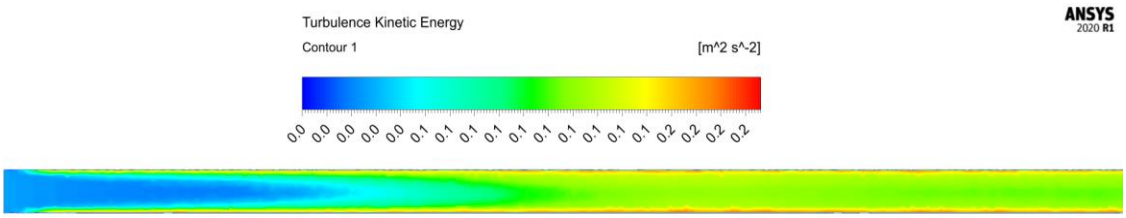

Figure 18a TKE for plain pipe at Re = 20000

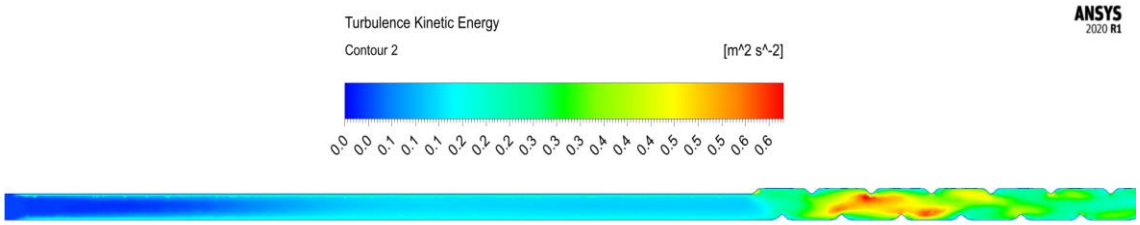

Figure 18b TKE for P12 using water at Re = 20000

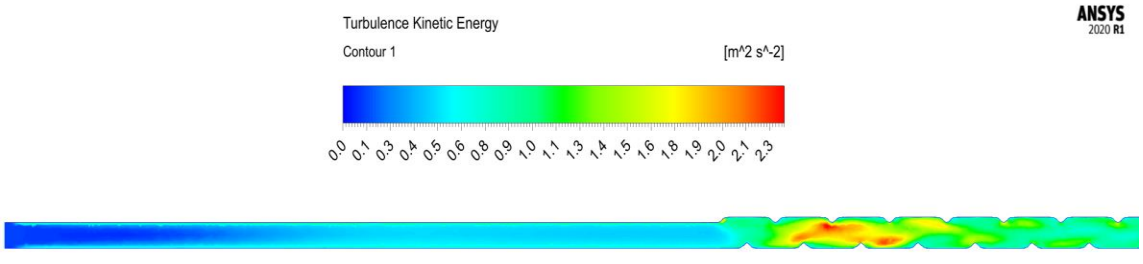

Figure 18c TKE for P12 using 1% Al2O3/Cu hybrid at Re = 20000

Chapter 7: Conclusion

In the current study, heat transfer characteristics for helically modified pipes were characterized for a constant heat flux having a fully turbulent flow regime (Re = 5000 to 20000), and it was investigated whether modifying certain geometric features of a corrugated tube (such as helical pitch and inlet corrugation shape) in combination with single phase nanoparticles and hybrid nanoparticles would enhance the heat transfer properties. The primary finding of this study is that employing hybrid nanofluids in modified geometries is a workable method for getting the best thermal performance, stimulating and simplifying heat exchanger design.

The key takeaways from this work may be summed up as follows:

• When compared to the results for plain tube, the corrugated design improves the Nusselt number at the price of a greater friction factor, increasing Nu and f by an average of 1.5 and 2 times, respectively.

• Higher pumping power is needed since the improved heat transfer performance comes at the expense of a pressure decrease.

• The corrugated pipe's heat transfer coefficient is determined to be 18.4% higher than the smooth pipe's at Re = 20,000 for using water as base fluid. The hybrid nanofluid is extremely efficient and has better thermal performance compared to water. A 1% Al2O3/Cu hybrid nanofluid's Nu and heat transfer coefficient are respectively around 24.3% and 29.2% higher than those of water at a Re of 20,000.

• Among the three case studies, the corrugated geometry with a trapezoidal shape inlet(P_{trap}) presented with the best PEC values whereas in terms of corrugation pitch, the configuration with the lower helical pitch(P12) gave better results.

• For each case study, the comparative improvement at lower Re number is greater than at larger Re number.

• Future work could be built on the validated test model by conducting additional parametric analysis on the corrugation shape, which determines the ideal geometrical variables and set of operating circumstances that optimize their performance in heat exchanger applications,

The creation of stable hybrid nanofluids and the development of new, less complex manufacturing techniques are the main objectives in this research. The compatibility of the at least two different types of nanoparticles that make up hybrid nanofluids is also a key factor. There is still much to learn about the various ways hybrid nanoparticles may be assembled, the stability of the suspensions, and the thermophysical characteristics of these systems.This method is a step in the right direction to determining the best cooling alternatives and aiming to overcome its difficulties brought on by the downsizing of electronic devices, even though the cost of creating hybrid nanofluid and its stability restrict it.

References:

[1] A. R. Al-Obaidi and J. Alhamid, "Numerical Investigation of Fluid Flow, Characteristics of Thermal Performance and Enhancement of Heat Transfer of Corrugated Pipes with Various Configurations," in *Journal of Physics: Conference Series*, Jan. 2021, vol. 1733, no. 1. doi: 10.1088/1742-6596/1733/1/012004.

[2] G. G. Cruz, M. A. A. Mendes, J. M. C. Pereira, H. Santos, A. Nikulin, and A. S. Moita, "Experimental and numerical characterization of single-phase pressure drop and heat transfer enhancement in helical corrugated tubes," *Int. J. Heat Mass Transf.*, vol. 179, Nov. 2021, doi: 10.1016/j.ijheatmasstransfer.2021.121632.

[3] T. Alam and M. H. Kim, "A comprehensive review on single phase heat transfer enhancement techniques in heat exchanger applications," *Renewable and Sustainable Energy Reviews*, vol. 81. Elsevier Ltd, pp. 813–839, Jan. 01, 2018. doi: 10.1016/j.rser.2017.08.060.

[4] P. Promvonge, S. Skullong, S. Kwankaomeng, and C. Thiangpong, "Heat transfer in square duct fitted diagonally with angle-finned tape-Part 1: Experimental study," *Int. Commun. Heat Mass Transf.*, vol. 39, no. 5, pp. 617–624, 2012, doi: 10.1016/j.icheatmasstransfer.2012.03.007.

[5] R. K. Ajeel, K. Sopian, R. Zulkifli, S. N. Fayyadh, and A. Kareem Hilo, "Assessment and analysis of binary hybrid nanofluid impact on new configurations for curved-corrugated channel," *Adv. Powder Technol.*, vol. 32, no. 10, pp. 3869–3884, 2021, doi: 10.1016/j.apt.2021.08.041.

[6] W. T. Ji, A. M. Jacobi, Y. L. He, and W. Q. Tao, "Summary and evaluation on single-phase heat transfer enhancement techniques of liquid laminar and turbulent pipe flow," *International Journal of Heat and Mass Transfer*, vol. 88. Elsevier Ltd, pp. 735–754, Sep. 01, 2015. doi: 10.1016/j.ijheatmasstransfer.2015.04.008.

[7] S. Pethkool, S. Eiamsa-ard, S. Kwankaomeng, and P. Promvonge, "Turbulent heat transfer enhancement in a heat exchanger using helically corrugated tube," *Int. Commun. Heat Mass*

Transf., vol. 38, no. 3, pp. 340–347, 2011, doi: 10.1016/j.icheatmasstransfer.2010.11.014.

[8] . M. M. E., "Investigation of Thermo-Fluid Behaviour of Nanofluid Through a Corrugated Tube," *Int. J. Res. Eng. Technol.*, vol. 05, no. 07, pp. 397–404, 2016, doi: 10.15623/ijret.2016.0507063.

[9] J. Alhamid and R. A. Al-Obaidi, "Flow Pattern Investigation and Thermohydraulic Performance Enhancement in Three-Dimensional Circular Pipe under Varying Corrugation Configurations," *J. Phys. Conf. Ser.*, vol. 1845, no. 1, 2021, doi: 10.1088/1742-6596/1845/1/012061.

[10] F. Ahmad, S. Mahmud, M. M. Ehsan, and M. Salehin, "Thermo-hydrodynamic performance evaluation of double-dimpled corrugated tube using single and hybrid nanofluids," *Int. J. Thermofluids*, vol. 17, no. October 2022, p. 100283, 2023, doi: 10.1016/j.ijft.2023.100283.

[11] A. Kaood and M. A. Hassan, "Thermo-hydraulic performance of nanofluids flow in various internally corrugated tubes," *Chem. Eng. Process. - Process Intensif.*, vol. 154, Aug. 2020, doi: 10.1016/j.cep.2020.108043.

[12] A. R. Al-Obaidi, "Investigation on effects of varying geometrical configurations on thermal hydraulics flow in a 3D corrugated pipe," *Int. J. Therm. Sci.*, vol. 171, no. August 2021, p. 107237, 2022, doi: 10.1016/j.ijthermalsci.2021.107237.

[13] Y. Chudnovsky and A. Kozlov, "Development and Field Trial of Dimpled-Tube Technology for Chemical Industry Process Heaters," *U.S. Dep. Energy Off. Sci. Tech. Inf.*, no. September, 2006.

[14] M. M. Ali and S. Ramadhyani, "Experiments on convective heat transfer in corrugated channels," *Exp. Heat Transf.*, vol. 5, no. 3, pp. 175–193, 1992, doi: 10.1080/08916159208946440.

[15] J. S. Jayakumar, S. M. Mahajani, J. C. Mandal, P. K. Vijayan, and R. Bhoi, "Experimental and CFD estimation of heat transfer in helically coiled heat exchangers," *Chem. Eng. Res. Des.*, vol. 86, no. 3, pp. 221–232, 2008, doi: 10.1016/j.cherd.2007.10.021.

[16] A. Verma, M. Kumar, and A. K. Patil, "Enhanced heat transfer and frictional losses in heat exchanger tube with modified helical coiled inserts," *Heat Mass Transf. und*

Stoffuebertragung, vol. 54, no. 10, pp. 3137–3150, 2018, doi: 10.1007/s00231-018-2347-x.

[17] H. Khosravi-Bizhaem, A. Abbassi, and A. Zivari Ravan, "Heat transfer enhancement and pressure drop by pulsating flow through helically coiled tube: An experimental study," *Appl. Therm. Eng.*, vol. 160, no. June, p. 114012, 2019, doi: 10.1016/j.applthermaleng.2019.114012.

[18] G. Zhang, Y. Li, D. B. Mohammed, and D. Toghraie, "Optimization of a high-temperature recuperator equipped with corrugated helical heat exchanger for improvement of thermal-hydraulic performance," *Case Stud. Therm. Eng.*, vol. 33, no. March, p. 101956, 2022, doi: 10.1016/j.csite.2022.101956.

[19] M. Salehin, M. Mehsan, A. Mehmood, M. Awais, and M. Usman, "INVESTIGATION OF TiO 2 -WATER NANOFLUID BEHAVIOR THROUGH A WAVY CORRUGATED PIPE IN TERMS OF HEAT," no. 8, pp. 35–40, 2016.

[20] M. Salehin, M. M. Ehsan, and A. K. M. Sadrul Islam, "Performance evaluation of nanofluid for heat transfer enhancement and pumping power reduction through a semicircular corrugated pipe," *Model. Meas. Control B*, vol. 86, no. 1, pp. 296–311, 2017, doi: 10.18280/mmc_b.860120.

[21] S. M. Mousazadeh, M. M. Shahmardan, T. Tavangar, K. Hosseinzadeh, and D. D. Ganji, "Numerical investigation on convective heat transfer over two heated wall-mounted cubes in tandem and staggered arrangement," *Theor. Appl. Mech. Lett.*, vol. 8, no. 3, pp. 171–183, 2018, doi: 10.1016/j.taml.2018.03.005.

[22] A. A. Hussien, M. Z. Abdullah, N. M. Yusop, M. A. Al-Nimr, M. A. Atieh, and M. Mehrali, "Experiment on forced convective heat transfer enhancement using MWCNTs/GNPs hybrid nanofluid and mini-tube," *Int. J. Heat Mass Transf.*, vol. 115, pp. 1121–1131, 2017, doi: 10.1016/j.ijheatmasstransfer.2017.08.120.

[23] M. Goodarzi *et al.*, "Boiling heat transfer characteristics of graphene oxide nanoplatelets nano-suspensions of water-perfluorohexane (C 6 F 14) and water-n-pentane," *Alexandria Eng. J.*, 2020, doi: 10.1016/j.aej.2020.08.003.

[24] A. A. Rabienataj Darzi, M. Abuzadeh, and M. Omidi, "Numerical investigation on thermal

performance of coiled tube with helical corrugated wall," *Int. J. Therm. Sci.*, vol. 161, no. December 2020, p. 106759, 2021, doi: 10.1016/j.ijthermalsci.2020.106759.

[25] T. Srinivas and A. Venu Vinod, "Performance of an agitated helical coil heat exchanger using Al2O3/water nanofluid," *Exp. Therm. Fluid Sci.*, vol. 51, pp. 77–83, 2013, doi: 10.1016/j.expthermflusci.2013.07.003.

[26] S. Biswakarma, S. Roy, B. Das, and B. Kumar, "Performance analysis of internally helically v-grooved absorber tubes using nano fl uid," *Therm. Sci. Eng. Prog.*, vol. 18, no. December 2019, p. 100538, 2020, doi: 10.1016/j.tsep.2020.100538.

[27] N. Abed, I. Afgan, A. Cioncolini, H. Iacovides, A. Nasser, and T. Mekhail, "Thermal performance evaluation of various nanofluids with non-uniform heating for parabolic trough collectors," *Case Stud. Therm. Eng.*, vol. 22, no. July, p. 100769, 2020, doi: 10.1016/j.csite.2020.100769.

[28] E. Bellos and C. Tzivanidis, "Thermal analysis of parabolic trough collector operating with mono and hybrid nanofluids," *Sustain. Energy Technol. Assessments*, vol. 26, no. August, pp. 105–115, 2018, doi: 10.1016/j.seta.2017.10.005.

[29] S. K. Singh and J. Sarkar, "Experimental hydrothermal characteristics of concentric tube heat exchanger with V-cut twisted tape turbulator using PCM dispersed mono/hybrid nanofluids," *Exp. Heat Transf.*, vol. 34, no. 5, pp. 421–442, 2021, doi: 10.1080/08916152.2020.1772412.

[30] A. Akhgar and D. Toghraie, "An experimental study on the stability and thermal conductivity of water-ethylene glycol/TiO2-MWCNTs hybrid nanofluid: Developing a new correlation," *Powder Technol.*, vol. 338, pp. 806–818, Oct. 2018, doi: 10.1016/j.powtec.2018.07.086.

[31] R. E. Ratul, F. Ahmed, S. Alam, M. Rezwanul Karim, and A. A. Bhuiyan, "Numerical study of turbulent flow and heat transfer in a novel design of serpentine channel coupled with D-shaped jaggedness using hybrid nanofluid," *Alexandria Eng. J.*, vol. 68, pp. 647–663, 2023, doi: 10.1016/j.aej.2023.01.061.

[32] J. A. Eastman, U. S. Choi, S. Li, G. Soyez, L. J. Thompson, and R. J. DiMelfi, "Novel

thermal properties of nanostructured materials," *Mater. Sci. Forum*, vol. 312, pp. 629–634, 1999, doi: 10.4028/www.scientific.net/msf.312-314.629.

[33] B. Takabi and H. Shokouhmand, "Effects of Al2O3-Cu/water hybrid nanofluid on heat transfer and flow characteristics in turbulent regime," *Int. J. Mod. Phys. C*, vol. 26, no. 4, pp. 1–25, 2015, doi: 10.1142/S0129183115500473.

[34] Y. Xuan and W. Roetzel, "Conceptions for heat transfer correlation of nanofluids," *Int. J. Heat Mass Transf.*, vol. 43, no. 19, pp. 3701–3707, 2000, doi: 10.1016/S0017-9310(99)00369-5.

[35] H. C. Brinkman, "The viscosity of concentrated suspensions and solutions," *J. Chem. Phys.*, vol. 20, no. 4, p. 571, 1952, doi: 10.1063/1.1700493.

[36] R. L. Hamilton, "Thermal conductivity of heterogeneous two-component systems," *Ind. Eng. Chem. Fundam.*, vol. 1, no. 3, pp. 187–191, 1962, doi: 10.1021/i160003a005.

[37] Ç. Yıldız, M. Arıcı, and H. Karabay, "Comparison of a theoretical and experimental thermal conductivity model on the heat transfer performance of Al2O3-SiO2/water hybrid-nanofluid," *Int. J. Heat Mass Transf.*, vol. 140, pp. 598–605, 2019, doi: 10.1016/j.ijheatmasstransfer.2019.06.028.

[38] M. Gürdal, H. K. Pazarlıoğlu, M. Tekir, K. Arslan, and E. Gedik, "Numerical investigation on turbulent flow and heat transfer characteristics of ferro-nanofluid flowing in dimpled tube under magnetic field effect," *Appl. Therm. Eng.*, vol. 200, no. June 2021, 2022, doi: 10.1016/j.applthermaleng.2021.117655.

[39] I. J. K. Wong and N. T. A. Tiong, "Simulation approach on turbulent thermal performance factor of Al2O3-Cu/water hybrid nanofluid in circular and non-circular ducts," *SN Appl. Sci.*, vol. 3, no. 3, pp. 1–15, 2021, doi: 10.1007/s42452-021-04317-w.

[40] C. Yang, G. Liu, J. Zhang, and J. yuan Qian, "Thermohydraulic analysis of hybrid smooth and spirally corrugated tubes," *Int. J. Therm. Sci.*, vol. 158, no. January, p. 106520, 2020, doi: 10.1016/j.ijthermalsci.2020.106520.

[41] M. H. Cheraghi, M. Ameri, and M. Shahabadi, "Numerical study on the heat transfer enhancement and pressure drop inside deep dimpled tubes," *Int. J. Heat Mass Transf.*, vol.

147, p. 118845, 2020, doi: 10.1016/j.ijheatmasstransfer.2019.118845.

[42] H. C. Kang, J. H. Eoh, J. E. Cha, and S. O. Kim, “Numerical study on pressure drop and heat transfer for designing sodium-to-air heat exchanger tube banks on advanced sodium-cooled fast reactor,” *Nucl. Eng. Des.*, vol. 254, pp. 5–15, 2013, doi: 10.1016/j.nucengdes.2012.08.003.

[43] A. García, J. P. Solano, P. G. Vicente, and A. Viedma, “The influence of artificial roughness shape on heat transfer enhancement: Corrugated tubes, dimpled tubes and wire coils,” *Appl. Therm. Eng.*, vol. 35, no. 1, pp. 196–201, 2012, doi: 10.1016/j.applthermaleng.2011.10.030.